UNIVERSIDADE ESTADUAL PAULISTA "JÚLIO DE MESQUITA FILHO"

Programa de Pós-graduação em Ciência e Tecnologia de Materiais (POSMAT)

César Augusto Antônio

DEPOSIÇÃO DE REVESTIMENTO BIOATIVO EM TITÂNIO POR OXIDAÇÃO ELETROLÍTICA COM PLASMA

SOROCABA

2018

César Augusto Antônio

DEPOSIÇÃO DE REVESTIMENTO BIOATIVO EM TITÂNIO POR OXIDAÇÃO ELETROLÍTICA COM PLASMA

Tese apresentada como requisito à obtenção de título de Doutor ao – Programa de Pós-Graduação em Ciência e Tecnologia de Materiais, área de concentração Ciência e Engenharia de Interfaces, sob a orientação do Prof. Dr. Nilson Cristino da Cruz.

SOROCABA

2018

ATA DA DEFESA PÚBLICA DA TESE DE DOUTORADO DE CESAR AUGUSTO ANTONIO, DISCENTE DO PROGRAMA DE PÓS-GRADUAÇÃO EM CIÊNCIA E TECNOLOGIA DE MATERIAIS , DA FACULDADE DE CIÊNCIAS - CÂMPUS DE BAURU.

Aos 12 dias do mês de setembro do ano de 2018, às 13:30 horas, no(a) Auditório do Câmpus de Sorocaba, reuniu-se a Comissão Examinadora da Defesa Pública, composta pelos seguintes membros: Prof. Dr. NILSON CRISTINO DA CRUZ - Orientador(a) do(a) Curso de Engenharia de Controle e Automação / Instituto de Ciência e Tecnologia/ UNESP/ Sorocaba, Profª Drª ADRIANA DE OLIVEIRA DELGADO SILVA do(a) Departamento de Física, Química e Matemática / Universidade Federal de São Carlos, Profa. Dra. ELAINE CONCEIÇÃO DE OLIVEIRA do(a) Faculdade de Tecnologia José Crespo Gonzales / Fatec - Sorocaba, Prof. Dr. DIEGO RAFAEL NESPEQUE CORRÊA do(a) Instituto Federal de São Paulo - Campus de Sorocaba, Prof. Dr. FRANCISCO TRIVINHO STRIXINO do(a) Departamento de Física, Química e Matemática / Universidade Federal de São Carlos - Centro de Ciências e Tecnologias para a Sustentabilidade, sob a presidência do primeiro, a fim de proceder a arguição pública da TESE DE DOUTORADO de CESAR AUGUSTO ANTONIO, intitulada **Deposição de Revestimento Bioativo em Titânio por Oxidação Eletrolítica com Plasma**. Após a exposição, o discente foi arguido oralmente pelos membros da Comissão Examinadora, tendo recebido o conceito final _APROVADO_ _ _ _ _. Nada mais havendo, foi lavrada a presente ata, que após lida e aprovada, foi assinada pelos membros da Comissão Examinadora.

Prof. Dr. NILSON CRISTINO DA CRUZ

Profª Drª ADRIANA DE OLIVEIRA DELGADO SILVA

Profa. Dra. ELAINE CONCEIÇÃO DE OLIVEIRA

Prof. Dr. DIEGO RAFAEL NESPEQUE CORRÊA

Prof. Dr. FRANCISCO TRIVINHO STRIXINO

Não importa quanto a vida possa ser ruim, sempre existe algo que você pode fazer, e triunfar. Enquanto há vida, há esperança.

Stephen Hawking

AGRADECIMENTOS

Agradeço a Deus pela força que tem dado e pelo livramento de um grande AVC (Acidente Vascular Cerebral) desde janeiro 2017.

À minha esposa, Silmara Alvarez Antônio, enorme companheira, que não mediu esforços para cooperar na realização deste trabalho e pela participação intensa no processo de recuperação de meu acidente.

Aos meus filhos, César Augusto Antônio Júnior e Kélvin Augusto Antônio, minhas fontes de inspiração, pela compreensão nas minhas ausências.

Aos meus pais, José Antônio (in memoriam) e Aparecida Machado pelo incentivo, apoio e por acreditar na realização deste trabalho.

Aos meus irmãos Luiz Carlos, Karen, Marcos, Heliete, Ana e Roseli e suas respectivas famílias pelo enorme carinho e união familiar.

Ao orientador Professor Dr. Nilson Cristino Cruz pelo enorme aprendizado e amizade, por ter me fornecido a oportunidade e confiança de poder fazer parte da equipe do LAPTEC, proporcionando conhecimento, apoio e participação intensa em todo o decorrer desta pesquisa.

À Professora Dra. Elidiane Cipriano Rangel pela amizade, consideração confiança, apoio, conhecimento, incentivo e por acreditar que seria capaz de realizar este projeto, mesmo nas horas mais difíceis ocorridas nesta etapa.

Ao técnico, mestre e doutorando Rafael Parra Ribeiro pelo enorme empenho na realização das análises das amostras.

À Professora Dra. Adriana de Oliveira Delgado pelo apoio em várias etapas deste trabalho.

À mestranda Tamires do Espírito Santo Araújo pela participação neste projeto desde a sua implantação/montagem dos equipamentos utilizados no processo PEO.

Ao Programa de Pós-Graduação de Ciência e Tecnologia de Materiais (POSMAT).

À toda equipe do LAPTEC pela amizade, aprendizado e companheirismo.

Ao prof. Dr. Manfredo Tabacniks pelas análises de RBS.

À profa. Dra. Eliana Duek pelas análises de crescimento celular e Fosfatase Alcalina.

À empresa Conexão pela doação das amostras.

RESUMO

O titânio e suas ligas, embora sejam biocompatíveis, não promovem o processo de diferenciação celular. Em consequência disto, diversas técnicas são empregadas para melhorar este requisito, como por exemplo, o recobrimento de sua superfície por uma camada de fosfato de cálcio, tal como a hidroxiapatita (HA). Porém processos atuais de deposição de fosfato necessitam de longos períodos de tratamento, elevadas temperaturas de deposição e posteriores tratamentos térmicos para cristalização do fosfato de cálcio, transformando-o em HA. Neste estudo, a técnica de Oxidação Eletrolítica com Plasmas (PEO) foi empregada para se depositar, sobre titânio Grau 4, revestimentos com altas concentrações de hidroxiapatita, em curtos períodos de tempos, sem a necessidade de pré ou pós-tratamentos. Também foi produzida HA dopada com magnésio, um importante nutriente para diferenciação celular, em uma única etapa de tratamento. Utilizou-se a técnica de difração de raios X (DRX) com Refinamento de Rietveld para identificar e quantificar as fases cristalinas presentes e a composição química dos revestimentos foi determinada empregando as espectroscopias de retro espalhamento Rutherford (RBS) e de energia dispersiva de raios X (EDS). A rugosidade e a morfologia das superfícies foram avaliadas por perfilometria e microscopia eletrônica de varredura (MEV), respectivamente. A difração de raios X revelou que foram depositados revestimentos com até 83,5% de HA e até 73,5% de HA dopada com Mg. Os resultados de adesão, proliferação e diferenciação celulares, por Fosfatase Alcalina, revelaram que os revestimentos contendo HA promoveram um aumento de até 43% na diferenciação celular, em comparação com o titânio sem tratamento.

Palavras-chave: Hidroxiapatita. Oxidação Eletrolítica com Plasma. Titânio. Revestimento Bioativo.

ABSTRACT

Although titanium and its alloys are biocompatible, they do not promote cell differentiation. As a consequence, various techniques are employed to improve this requirement. In this sense, one of the most important approach is the coating of its surface by a layer of calcium phosphate, such as hydroxyapatite (HA). However, current phosphate deposition processes require long treatment time, high deposition temperatures and subsequent thermal treatments for crystallization of calcium phosphate, transforming it into HA. In this study, Plasma Electrolytic Oxidation (PEO) technique has been used to deposit, on Grade 4-Titanium samples, coatings with high concentrations of hydroxyapatite, in short periods of time, without the need for pre or post treatments. Furthermore, magnesium, an important nutrient for cell differentiation, was incorporated in HA coatings in a single treatment step. X-ray diffraction (XRD) with Rietveld refinement was used to identify and quantify the crystalline phases. The chemical composition of the coatings was determined using Rutherford backscattering (RBS) and X-ray dispersive energy (EDS) spectroscopies. Surface roughness and morphology were evaluated by profilometry and scanning electron microscopy (SEM), respectively. X-ray diffraction revealed that some coatings contained up to 83.5% HA and up to 73.5% Mg doped HA. Cell adhesion, proliferation and differentiation results, by Alkaline Phosphatase, revealed that HA-containing coatings promoted an increase in up to 43% in cell differentiation compared to untreated titanium.

Keywords: Hydroxyapatite. Plasmas Electrolytic Oxidation. Titanium. Bioactive Coating.

SUMÁRIO

INTRODUÇÃO

O titânio e suas ligas são metais largamente usados na fabricação de implantes dentários e ortopédicos por possuírem propriedades tais como módulo de elasticidade relativamente baixo, boa resistência à fadiga, conformabilidade, usinabilidade, resistência à corrosão e biocompatibilidade. No entanto, os implantes com tais metais são bioinertes, ou seja, não estimulam a osseointegração, que é a capacidade de promover a transformação de células osteoblásticas em osso. Este aspecto pode ser melhorado a partir da formação de revestimentos como, por exemplo, uma camada de fosfato de cálcio, como a hidroxiapatita (HA, $Ca_{10}(PO_4)_6OH_2$), que compõe cerca de 70% do osso humano, que torna a superfície do implante bioativa e com ótima funcionalidade in vivo. A HA sintética é semelhante ao mineral ósseo e dentário, com boa bioatividade e biocompatibilidade (Halouani,1994 e Thomas, 1981). Desta forma, quando produzida sinteticamente sobre o implante, promove boa ligação química com o tecido ósseo corpóreo (Fatehi, 2008).

Interessantes propriedades biológicas das HA produzidas sinteticamente têm sido alcançadas. Porém, a busca por maior similaridade da HA do osso nativo com a sintética tem motivado o desenvolvimento de técnicas que possibilitem obter HA cada vez mais bioativa (Elliott, 2013 e Mayer, 2000). Neste sentido, diversas técnicas podem ser empregadas para a produção de revestimentos contendo hidroxiapatita. Lewis (2017), por exemplo, depositou HA utilizando a técnica de plasma spray. Embora esta seja a única técnica comercialmente empregada, ela demanda tratamentos térmicos em temperaturas que podem ultrapassar 1000° C por períodos superiores a 60 minutos. Tais temperaturas elevadas podem promover distorções dimensionais e delaminação dos revestimentos. Além disto, para se depositar HA por Plasma spray é necessário que o substrato seja previamente submetido a um jato de gás a alta velocidade contendo partículas de algum material duro, como a alumina, por exemplo, para aumentar a rugosidade superficial. Após este preparo ocorre a deposição dos revestimentos que se dá pela condensação de partículas de fosfato de cálcio lançadas sobre a superfície por um jato de plasma (um gás aquecido pela passagem de corrente elétrica). Algumas desvantagens desta técnica, incluem

tempos de deposição prolongados e a necessidade de submissão dos implantes a processos de tratamentos térmicos em temperaturas entre 600° a 700° C, por um tempo mínimo de duas horas, para melhorar a cristalinidade da HA. Recentemente, Domínguez-Trujillo et al (2018) produziram HA em titânio poroso a partir da técnica Sol-Gel. Para tanto, foi necessária a imersão em solução de Fosfato de Trietila ($C_6H_{15}O_3P$) e Nitreto de Cálcio (Ca_3N_2) hidrolisado por 24 horas, seguido por tratamento térmico a 450° C durante 5 horas em um forno à vácuo. Esse processo além de ser composto por várias etapas, demanda ao menos 30 horas para a finalização.

Apatitas biológicas não são de composição estequiométrica, possuem baixa cristalinidade e muitas vezes contêm impurezas iónicas, tais como Zn^{+2}, Mg^{+2}, Na^+, CO_3^{-2}, e F (Narasaraju, 1996). Estes elementos iônicos incorporados à HA desempenham um papel significativo no metabolismo ósseo, tais como crescimento e absorção de nutrientes. Por esta razão, a incorporação de elementos iônicos nas apatitas sintéticas é considerada relevante para promover melhores propriedades biológicas e a busca pela similaridade ao osso natural (Yerokhin, 2000 e Adamopoulos, 2007). Dentre estes elementos que podem ser incorporados à HA, o magnésio é amplamente estudado, sendo um dos íons mais importantes para manutenção da saúde dos ossos. É o quarto elemento mais abundante no corpo humano e auxilia na diminuição da cristalização, reduz o tamanho do cristal e diminui a proliferação e a atividade de células semelhantes a osteoblastos (Marchi, 2009 e Sharifnabi, 2015). Sua deficiência afeta todas as etapas do metabolismo esquelético levando a inibição do crescimento ósseo, diminuindo as atividades osteoblásticas e osteoclásticas e causando fragilidade ao osso (Fini, 2003 e Chen, 2005). Em consequência disto, investiga-se também os efeitos da incorporação deste nutriente aos revestimentos de hidroxiapatita. Usualmente isto é feito em duas etapas. Na primeira delas é realizada a deposição de HA pelos processos convencionais, como o plasma spray, por exemplo, e, posteriormente, faz-se a dopagem da HA, tipicamente com processos de difusão em via úmida, seguido de tratamentos térmicos. Stipniece (2014), por exemplo, obteve a dopagem da HA através da imersão das amostras em solução contendo Mg por um período para estabilização dos implantes na solução e posterior secagem pela submissão das amostras à temperatura de 105° C por 20

horas. Procedimento semelhante foi empregado por Aneta Zima (2017), que obteve a incorporação de magnésio através da precipitação de íons de Mg em amostras contendo HA imersas em solução fisiológica por 24 h a temperatura ambiente. A técnica de deposição a Laser Pulsado (PLD) foi utilizada para depositar hidroxiapatita dopada com Mg por Mroz et al (2009), em uma amostra de titânio recoberta por Nitreto de Titânio (TiN). Foram produzidas camadas com 3 μm de espessura a partir da deposição, durante 35 minutos, à base de fosfato de cálcio. Após esse procedimento, a hidroxiapatita foi obtida por processos em via úmida. Assim, para produzir hidroxiapatita dopada com magnésio foram necessárias várias etapas (Mroz et al, 2010). Neste contexto, uma técnica com grande potencial, mas ainda pouco explorada é a Oxidação Eletrolítica assistida por Plasmas (PEO) (Yerokhin, 2000), que combina os efeitos da oxidação eletrolítica convencional com micro-arcos elétricos que surgem na amostra quando a tensão aplicada nos eletrodos ultrapassa algumas centenas de volts. Este método tem sido usado para produzir revestimentos cerâmicos em metais leves tais como Ti, Al, Nb, Ta e Mg (HEANEY, 2006).

OBJETIVOS GERAIS E ESPECÍFICOS

Após uma extensa busca na literatura especializada, considerando artigos publicados entre 2011 e 2018, não foram encontrados estudos, além dos apresentados neste trabalho, com a finalidade de produzir HA pela técnica PEO com a incorporação de Mg. Sendo assim para contribuir com a redução da carência de informações nesta área, o presente trabalho objetivou a produção de revestimentos com elevada quantidade de HA e em curtos períodos de deposição sobre a liga de titânio Grau 4. Após alcançados relevantes resultados na deposição do revestimento com hidroxiapatita, buscou-se a incorporação de magnésio aos revestimentos em uma única etapa.

Alguns dos principais resultados obtidos neste trabalho foram publicados em dois artigos apresentados e brevemente discutidos a seguir.

PROCEDIMENTO EXPERIMENTAL

Discos de Titânio Grau 4 foram gentilmente cedidos pela empresa Conexão com 8 mm de diâmetro e 2 mm de espessura. Os tratamentos foram realizados em cuba de aço inoxidável (Fig. 1) equipada com um sistema de refrigeração e conectada ao terminal negativo de uma fonte de alta tensão pulsada. Todos os tratamentos foram realizados no modo potenciostático com pulsos de 480 V, 120 Hz, ciclo de trabalho de 60% e densidade média de corrente de 1,7 A/cm². O tempo de tratamento foi variado entre 120 e 600 s. A solução eletrolítica foi preparada dissolvendo-se 0,2 mol de Acetato de Cálcio e 0,2 mol de glicerofosfato de sódio em 1 litro de água deionizada.

Com o objetivo de dopar a HA com magnésio, os tratamentos foram realizados por 120 s acrescentando em condições semelhantes à descrita anteriormente acrescentando-se acetato de magnésio ao eletrólito em proporções variando de 0,2 a 0,8 mol.

Figura 1: Ilustração esquemática da cuba eletrolítica.
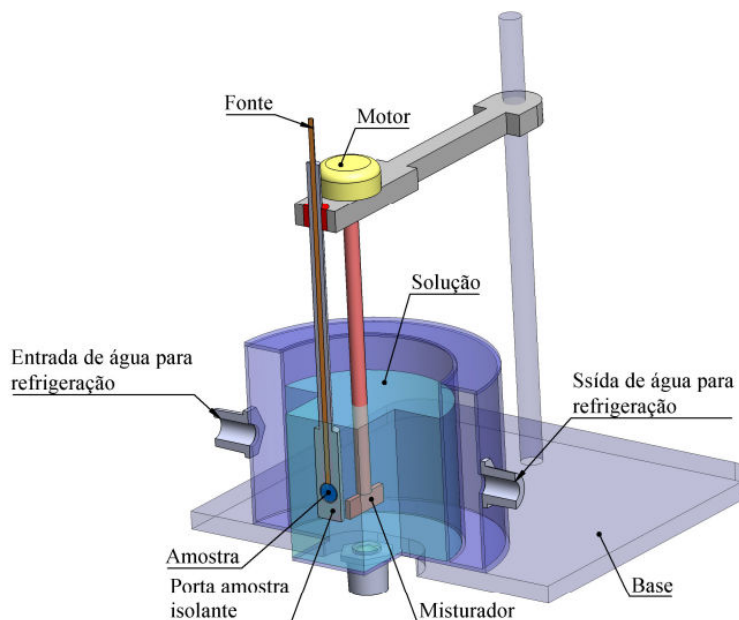
Fonte: Autor.

A composição química das amostras foi analisada por Espectroscopia de retroespalhamento de Rutherford (RBS) usando um feixe de hélio de 3,29 MeV e carga total de 10 µC. Perfis de composição e profundidade elementar foram determinados

por simulações computacional com softwares RUMP 52 e SIMNRA 53 (MAYER, 2000). As fases cristalinas dos revestimentos foram determinadas por Difração de Raios X obtidos com o equipamento da marca Panalytical X-Pert PRO, em geometria Ɵ - 2Ɵ, empregando radiação Cu-Kα (λ = 1,54 Å). A aquisição de dados foi realizada em ângulos de difração entre 20° e 60° em passos de 0,02° e 5 segundos por passo. A técnica de refinamento de Rietveld foi empregada para determinar a proporção de cada fase, bem como parâmetros de rede da célula cristalina da hidroxiapatita. O refinamento foi realizado usando o software X'Pert HighScorePlus com o modelo estrutural (banco de dados ISCD). A espessura das amostras foi determinada pelo corte e preparação metalográfica da secção transversal que evidenciou o revestimento, possibilitando a realização das medidas em microscópio eletrônico de varredura (JEOL – JSM 6010). Este microscópio também foi empregado no modo de elétrons retroespalhados com tensão de aceleração de 5 kV para investigar-se a morfologia superficial das amostras. A rugosidade foi determinada por perfilometria, usando um perfilômetro Profiler Veeco, Destak 150.

Artigo 1

Hydroxyapatite Coating Deposited on Grade 4 Titanium by Plasma Electrolytic Oxidation

César Augusto Antônio[a]*, Nilson Cristino Cruz[a], Elidiane Cipriano Rangel[a],

Rita de Cássia Cipriano Rangel[a], Tamires do Espirito Santo Araujo[a], Steven Frederick Durrant[a],

Bruna Antunes Más[b], Eliana Aparecida Rezende Duek[c]

[a]*Technological Plasmas Laboratory, Paulista State University – UNESP,
Experimental Campus of Sorocaba, Sorocaba, SP, Brazil*
[b]*Department of Material Engineering, Faculty of Mechanical Engineering,
Campinas State University – UNICAMP, Campinas, SP, Brazil*
[c]*Laboratory of Biomaterials, Pontifícia Universidade Católica de São Paulo – PUC-SP,
Sorocaba, SP, Brazil*

The present study reports the deposition of coating using Plasma Electrolytic Oxidation (PEO) onto grade 4 titanium to produce novel surface features. Samples were treated in an electrolytic solution of calcium acetate and sodium glycerolphosphate. The temporal evolution of hydroxyapatite coatings with high Ra roughness and a maximum thickness of 120 μm was obtained. X-ray spectra revealed the presence of hydroxyapatite, rutile and calcium phosphate. Cell growth measurement by MTT assay showed that the coatings were not toxic because cells grew on all samples.

Keywords: *Plasma Electrolytic Oxidation (PEO), hydroxyapatite, titanium*

1. Introduction

Titanium is widely-used as a biomaterial because it is biocompatible, chemically inert, and possesses good mechanical properties. It is not an ideal material from a medical standpoint as it does not present good bioactivity, i.e. bone does not grow spontaneously around it when implanted in the human body[1-3]. We are conducting studies to improve the bioactivity of this material.

Currently, there are two main lines of research focused on improving the bioactivity of titanium through changes in it is surface properties. These are based on the growth of a layer of hydroxyapatite, $Ca_{10}(PO_4)_6(OH)_2$, the principal mineral component of bone, on the metal surface. Hydroxyapatite (HA) has superior biocompatibility to any other known material[4]. Many studies propose the modification of the titanium surface to accelerate the spontaneous precipitation of apatite when in contact with the body; others propose the deposition of an HA layer.

The layer deposition techniques used to produce calcium phosphate include "plasma spray"[5-8], laser ablation, "magnetron sputtering"[9,10], sol-gel[11-14], electrophoresis[15,16], and biomimetic methods[17-19]. In the latter technique, the hydroxyapatite is precipitated from a saturated calcium phosphate solution, similar to that of blood. Among the techniques mentioned above, the only one commercially available is plasma spray, but the layers produced present problems. The connection between the hydroxyapatite and metal is purely mechanical, without chemical interaction between the two materials. Consequently, coatings behave as a brittle ceramic, presenting a low resistance to fatigue,

delamination and degradation when used in implants for prolonged periods[20,21]. The particles released into body can cause inflammatory reactions[22].

An alternative for the production of highly adherent layers using a cheap and simple methodology is Plasma Electrolytic Oxidation (PEO). Using PEO coatings can be deposited onto samples from an aqueous electrolyte, by applying a potential of a few hundred volts, which generates localized discharges on the sample surface[23]. The electrolytes dissolved in water dissociate to form anions and cations. When a voltage is applied between the electrodes, anions and cations are attracted to the anode and cathode, respectively. Thus, at the anode, the oxidation process begins. Initially, an insulating layer formed on the anode causes a significant drop in system current. With the increase of the applied voltage, the current is forced to pass through the coating. Intense electric fields around the samples generated localized electrical discharges, called micro-arcs. The coating is formed by oxidation of the samples and by deposition of elements from the electrolytic solution. As the micro-arcs produce high temperatures the oxide layer can be sintered and incorporate elements into the coating. The coating is deposited across the whole surface immersed in the solution. An improvement in adhesion of these layers is observed compared to that of hydroxyapatite layers deposited by plasma spray[24,25]. In addition, the layers are porous and rough, and resistant to wear and corrosion[26,27], which are interesting features for good bioactivity.

Recent studies have demonstrated the possibility of the deposition of HA films by PEO[28-32]. The different concentrations of calcium and phosphorus and the different

*e-mail: cesar.augustoa@hotmail.com

structures of these films are easily controlled by varying the concentration of the reagents used and the pH of the electrolyte solution[28]. Reagents commonly used for the electrolyte solution are tripolyphosphate, calcium acetate, calcium glycerophosphate, monosodium phosphate, and trisodium phosphate[29,31]. Some results show that it is possible to deposit various phases of calcium phosphate, including hydroxyapatite[30,32].

Currently, the formation of HA in coatings produced by PEO is possible using long treatment times together with high polarization frequencies. As confirmed by XRS, however, the amount of HA produced is small. Thus, the objective of this work is to obtain a coating containing a significant amount of HA using short depositions times.

2. Experimental Description

Grade 4 titanium disks of 8 mm diameter and 2 mm thickness were produced. After machining and polishing, the samples were sterilized and stored in suitable containers. The samples treatment was carried out in a stainless steel tank of capacity 2 l. The tank was enclosed in a cooling system that maintains the temperature of the solution at approximately 50 °C. The sample was attached at the anode and the tank served as the cathode itself. The electrolytic solution used for the treatment was 0.2 M calcium acetate (($CH_3COO)_2Ca$) and 0.02 M sodium glycerophosphate ($C_3H_5(OH)_2PO_4Na$) diluted in 1 liter of deionized water. The samples were treated with a current density that varied between 1.7 and 0.6 A cm^{-2} (both ± 0.2 A cm^{-2}) for times of 120, 300 and 600 s. The voltage, frequency and duty cycle were 480 V, 100 Hz and 60%, respectively. Treatment of the samples was carried out in the potentiostatic mode, during which the voltage is maintained constant and the current varies as a function of time. After PEO treatment, the samples were cleaned with deionized water and dried.

In this study, we investigated the structure, thickness, roughness, morphology, chemical composition and cytocompatibility of the coating. The coating thickness was measured by scanning electron microscopy (SEM) after preparation of a metallographic sample section. Sample surface roughness was verified by profilometry. SEM was used to analyze the morphology of the coating. X-ray diffraction using Cu-K_a radiation (λ = 1.54 Å) with angles between 20 and 60° and a step-size of 0.1°/ min, was used to examine the phase of the coating.

The cytocompatibility, i.e. the ability of the samples to support adhesion and cell growth of primary osteoblasts after 24 hours and 5 days of culture, was assessed using the colorimetric MTT metabolism assay (3 - (4,5-dimethylthiazol-2-yl) -2,5 diphenyl tetrazolium bromide). Osteoblasts were obtained by extraction from calvariae of three 20-day-old Wistar rats according to Declercq et al.[33]. Osteoblasts were cultured in Dulbecco's modified essential medium (DMEM) supplemented with 10% (v/v) heat-inactivated fetal bovine serum (FBS), gentamicin (50 µg/mL) and amphotericin B (5 µg/mL). The cells were then harvested using trypsin/EDTA and seeded onto 48-well culture plates containing the samples. The culture medium was changed every 2 days. For the MTT assay, 1x10^{3} cells/mL were seeded in wells containing the

samples. After 24 hours and 5 days of culture, the culture medium was removed and the wells washed twice with 0.1 M PBS, pH 7.4, at 37 °C, followed by the addition of 200 µL of DMEM and MTT reagent (20 µL/well, containing 5 mg of MTT reagent/mL). After incubation for 4 h at 37 °C, the cells were lysed by adding 200 µL of dimethylsulphoxide (DMSO). Subsequently, 100 µL aliquots of the solution in each well were transferred to a new plate and the absorbance then measured at 570 nm using a microplate reader. The data for the cytocompatibility assay was expressed as the mean ± standard deviation (SD) for n = 4 experiments. Analysis of variance (One-Way ANOVA) followed by the Tukey test (with p < 0.05) was used to assess the significance of the data. For the data analyses the BioEstat® 5.0 statistical software was used.

3. Results and Discussion

3.1. Current density characteristics

When the supply is turned on, the voltage between the electrodes rises automatically to 480 V in 10 s. At this treatment voltage, the sample surface is entirely covered by micro-arcs and the formation of the coating begins. The current, however, varies as function of treatment time since the coating growing on the titanium is electrically isolated, which changes the electrical conductivity of the system. Consequently, as shown in Figure 1, the current density varied from 1.7 to 0.6 Acm^{-2} (both ± 0.2 A cm^{-2}). Up to 50s of treatment time there is a rapid fall in the current density; subsequently, it falls at a lower rate.

3.2. Thickness and roughness

The coating growth process occurs both by sample oxidation and by incorporation of the species present in the electrolytic solution. In both of these processes recombination of species occurs, forming new materials on the treated sample surface. Figure 2 shows micrographs obtained by scanning electron microscopy (SEM) of transverse sections of samples treated using PEO. From these, the average coating thickness was 22, 135 and 120 µm, respectively. Observe that the thickness of the sample treated for 600 s is less than treated to 300 s. This may be due to ejection of material from the coating caused by high density micro-arcs.

Observation of the transverse section of the coating reveals that it is formed by a heterogeneous and porous layer. The large thickness shows that the coating completely covers the titanium.

An analysis of Figure 1 reveals that the current density initially falls rapidly, but at greater treatment times it falls at lesser rate. As the coating thickness increases, the electrical resistance of the system increases. Consequently, as the electric field is high near the samples, the more intense electrical discharge leads to the formation of high intensity micro-arcs. Thus, deposited material is ejected from the growing coating.

The rougness values are expressed as the average and the standard deviation of three measurements. Figure 3 shows that the roughness Ra increases with increasing treatment time. This increase is also justified by the action of micro-
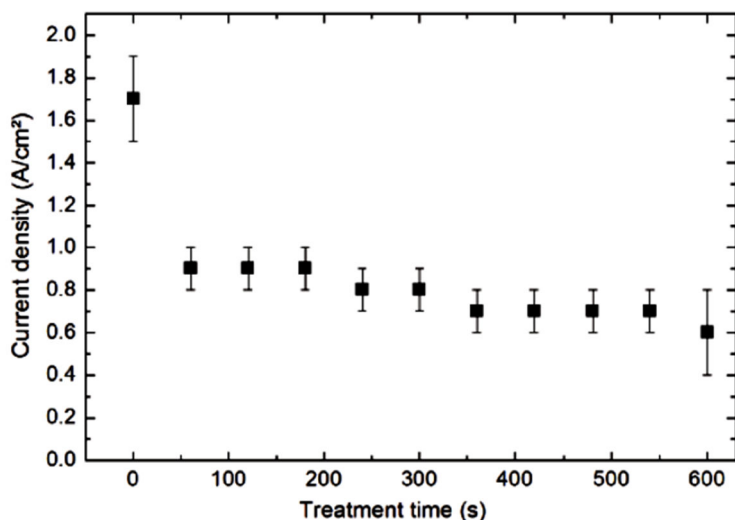
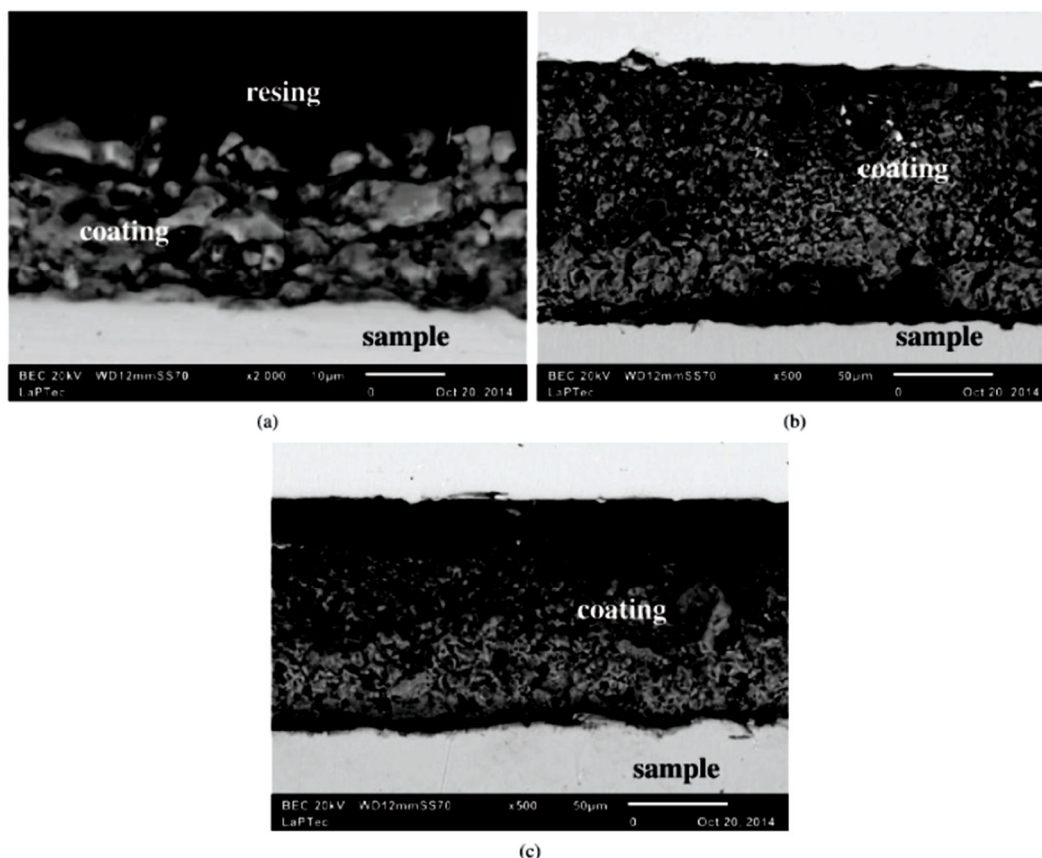**Figure 1.** Current density as a function of treatment time.

Figure 2. SEM micrograph, of the section of the titanium samples treated by PEO for different periods of time: (a) 120 s with magnification of 200x, (b) 300 s with magnification of 500x (c) 600 s with magnification of 500x.

arcs. The sample treated for 600 s has a greater roughness. Long treatment times generate more intense micro-arcs. The action of these micro-arcs increases the roughness of the samples by ejection of already-deposited material. Inspection of the standard deviation of the roughness of the sample treated for 600 s shows that the surface roughness is not uniform in the sample.

3.3. Morphology of the coating

The morphology of the samples treated by PEO may be observed in Figure 4. Inspection of Figure 4(a) shows that a new structure forms on the porous matrix. As the treatment time increases this structure grows and covers the porous matrix. At a treatment time of 300 s, the structure grows to form of clusters with tridimensional columns. It may also

be observed that the morphology of the layer is irregular, which explains the observed increase in roughness.

3.4. X-ray diffraction

The coatings produced by PEO, at a voltage of 480 V, on the titanium substrate are composed of HA, rutile and calcium phosphate ($Ca_2P_2O_7$). The spectrum of the samples treated for 120 s, presented in Figure 5, has well-defined
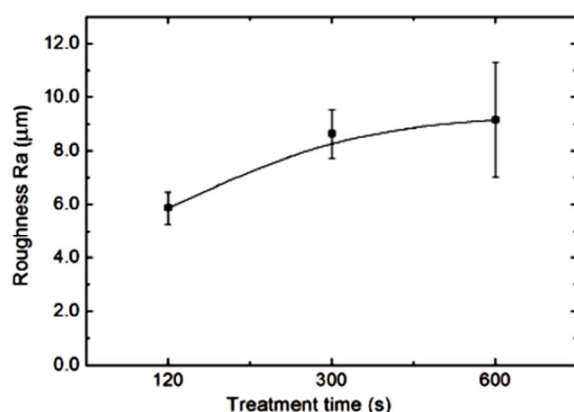

Figure 3. Sample roughness of titanium treated by PEO in different time.

peaks due to rutile and HA. Calcium phosphate is also detected, but the peaks have low intensities.

As the treatment time is increased the rutile phase disappears and the coating is composed only of HA and calcium phosphate. The peaks due to HA and calcium phosphate of the sample treated for 300 s have increased intensities compared to these of the spectrum of the sample treated for 120 s. Figure 4(a) shows that on the porous matrix a new cluster-like structure grows and as time passes the matrix is completely covered. Probably, the matrix bound to the titanium substrate is composed of rutile and the phase that covers the matrix is composed of HA and calcium phosphate. This interpretation is based on the observation that as the treatment time is increased rutile is no longer observed in the X-ray spectra. The first layers formed are more susceptible to the presence of rutile, since rutile is formed by the oxidation of titanium from the substrate.

As the coatings grow and the supply of titanium for production of rutile is interrupted HA and calcium phosphate predominate. Hence the clusters formed in the porous matrix (Figure 4) are made of HA.

Note that there are no significant differences between the spectra of samples treated for 300 and 600 s, except for a slight reduction in the intensity of peaks due to HA. To obtain HA in the coating, therefore, a time of 300 s is sufficient.
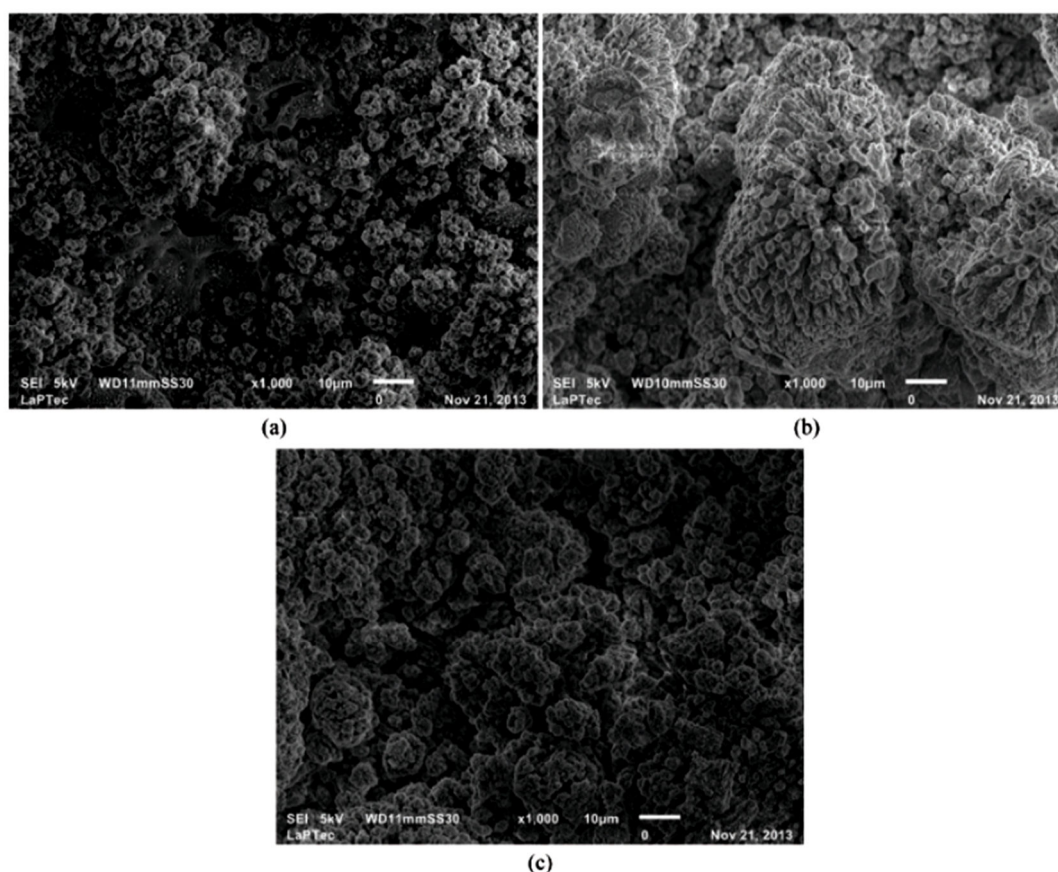

Figure 4. SEM micrograph, with magnification of 1000x, of titanium treated by PEO for different periods of time: (a) 120 s, (b) is 300 (c) 600 s.

No peak due to titanium metal is observed in the spectrum of the coating, which demonstrates the complete coverage of the samples surface.

3.5. Cell viability

The cytocompatibility of the HA coated-titanium samples after 120s, 300s and 600s of coating time was assessed by MTT assay, which is based on the ability of viable cells to reduce yellow 3-(4, 5-dimethythiazol-2-yl)-2, 5-diphenyl tetrazolium bromide (MTT) by mitochondrial succinate dehydrogenase. Since osteoblasts are anchorage-dependent cells and only metabolically active osteoblasts can attach to a substrate, the MTT results were interpreted as a measure of cellular adhesion and proliferation.

Figure 6 shows that samples treated by PEO, regardless of coating time, allowed cells to adhere to the sample surface

after 24h of culture ($p > 0.05$). No statistical differences were found among the samples in comparison with tissue culture on untreated Ti, which were used as a control ($p > 0.05$).

After 5 days of culture, it is observed in Figure 6 that all samples significantly stimulated cellular growth in relation to 24h of culture time ($p < 0.05$). Among the HA coated samples, no statistically significant differences in cell densities were found ($p > 0.05$); however, the amount of viable cells found in the samples coated for 600s was lower than those found in uncoated Ti samples ($p < 0.05$).

It has been shown that coating of HA onto implantable surfaces enhances osteoblast affinity, improving cell adhesion and proliferation[34,35]. In the present study, however, these results were not confirmed. On the other hand, although cytocompatibility of the coated samples was not
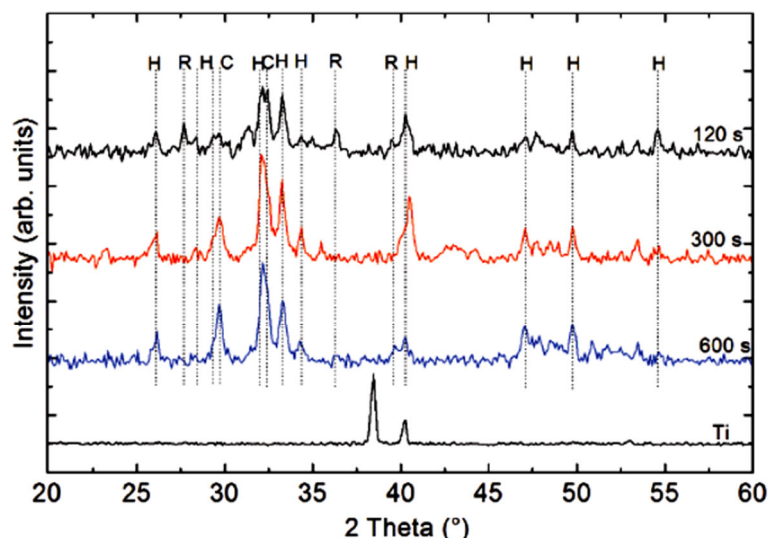

Figure 5. XRD patterns of coating produced by plasma electrolytic oxidation for different times, where H – Hydroxyapatite ($Ca_5(PO_4)_3$ (OH); C – Calcium Phosphate ($Ca_2P_2O_7$) and R – Rutile (TiO_2).
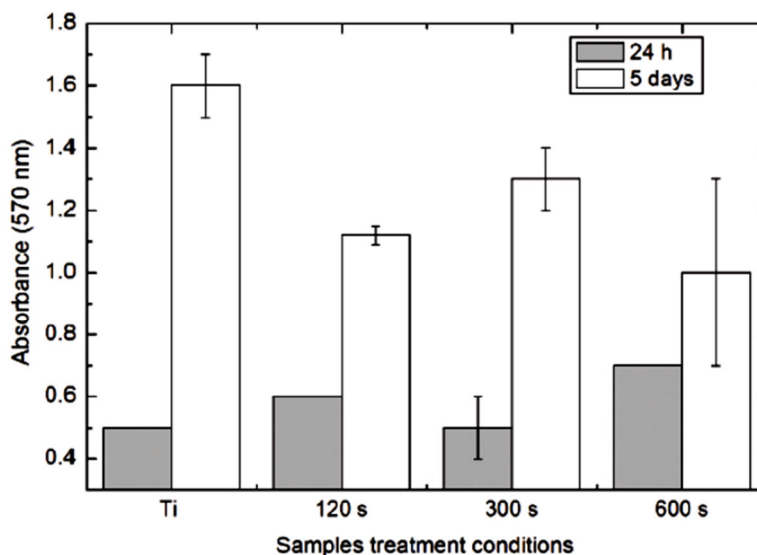

Figure 6. Cellular viability assay on specimens grown for growth times of 24 hours and 5 days. (The mean absorbance values and the standard deviation are given).

impaired for cell adhesion and proliferation, it was not significantly improved.

Similar results were reported by Yeung et al.[36], who assessed the cytocompatibility of PEO coated TiO_2 with human osteosarcoma cells (MG-63s) and found that PEO coated samples had fewer viable cells in comparison with plasma-sprayed HA samples and TCPS. The same authors believe that cellular behavior may be inhibited by the specific morphology or chemical composition of the PEO coating[36].

For 5 days of cultivation, the sample treated for 600 s was the only that presented cellular growth significantly less than the untreated sample, which was used as a control to compare with the treated samples (p <0.01). The sample treated for 600 s presented detachment of the deposited material, due to smaller thickness than the sample treated for 300 s. The standard deviation of the roughness shows that the surface was strongly affected by exposure of the sample to a long treatment time. The chemical composition and surface topography may have reduced the coating stability, which promoted less cell growth.

In general we can say that the treated samples are cytocompatible and stimulate significant cellular growth.

4. Conclusion

In this study, coatings composed of HA, rutile and calcium phosphate were produced from a solution containing a source of Ca and P. The main results are given below.

Using PEO it was possible to produce a porous coating composed of HA, rutile and calcium phosphate, possessing a high surface roughness; the latter property is useful for biomedical applications.

In one step, with a treatment time of 120 s, it was possible to obtain a coating containing HA. The HA phases depend on the treatment time, but samples treated for 120 s already present interesting characteristics for biomedical applications.

The coatings produced at all treatment times studied are cytocompatible.

Acknowledgments

References

1. Hanawa T and Ota M. Calcium phosphate naturally formed on titanium in electrolyte solution. *Biomaterials*. 1991; 12(8):767-774. http://dx.doi.org/10.1016/0142-9612(91)90028-9. PMid:1799652

2. Liu X, Poon RWY, Kwok SCH, Chu PK and Ding C. Structure and properties of Ca-plasma-implanted titanium. *Surface and Coatings Technology*. 2005; 191(1):43-48. http://dx.doi.org/10.1016/j.surfcoat.2004.08.118.

3. Hanawa T. In vivo metallic biomaterials and surface modification. *Materials Science and Engineering A*. 1999; 267(2):260-266. http://dx.doi.org/10.1016/S0921-5093(99)00101-X.

4. Ghomi H, Fathi MH and Edris H. Preparation of nanostructure hydroxyapatite scaffold for tissue engineering applications. *Journal of Sol-Gel Science and Technology*. 2011; 58(3):642-650. http://dx.doi.org/10.1007/s10971-011-2439-2.

5. Yang CY, Wang BC, Lee TM, Chang E and Chang GL. Intramedullary implant of plasma-sprayed hydroxyapatite coating: an interface study. *Journal of Biomedical Materials Research*. 1997; 36(1):39-48. http://dx.doi.org/10.1002/(SICI)1097-4636(199707)36:1<39::AID-JBM5>3.0.CO;2-M. PMid:9212387

6. Ong JL, Carnes DL and Bessho K. Evaluation of titanium plasma-sprayed and plasma-sprayed hydroxyapatite implants in vivo. *Biomaterials*. 2004; 25(19):4601-4606. http://dx.doi.org/10.1016/j.biomaterials.2003.11.053. PMid:15120505

7. Garcia-Alonso D, Parco M, Stokes J and Looney L. Low-Energy Plasma Spray (LEPS) Deposition of Hydroxyapatite/Poly-ε-Caprolactone Biocomposite Coatings. *Journal of Thermal Spray Technology*. 2012; 21(1):132-143. http://dx.doi.org/10.1007/s11666-011-9695-0.

8. Singh G, Singh S and Prakash S. Surface characterization of plasma sprayed pure and reinforced hydroxyapatite coating on Ti6Al4V alloy. *Surface and Coatings Technology*. 2011; 205(20):4814-4820. http://dx.doi.org/10.1016/j.surfcoat.2011.04.064.

9. Wang C, Chen Z, Guan L, Liu Z, Wang P, Zheng S, et al. Structural characterization of ion beam sputter deposited calcium phosphate coatings. *Surface and Coatings Technology*. 2000; 130(1):39-45. http://dx.doi.org/10.1016/S0257-8972(00)00705-2.

10. Bagratashvili VN, Antonov EN, Sobol EN, Popov VK and Howdle SM. Macroparticle distribution and chemical composition of laser deposited apatite coatings. *Applied Physics Letters*. 1995; 66(19):2451. http://dx.doi.org/10.1063/1.113992.

11. Lee J and Aoki H. Hydroxyapatite coating on Ti plate by a dipping method. *Bio-Medical Materials and Engineering*. 1995; 5(2):49-58. PMid:7655318.

12. Li P, De Groot K and Kokubo T. Bioactive Ca10(PO4)6(OH)2-TiO2 composite coating prepared by sol-gel process. *Journal of Sol-Gel Science and Technology*. 1996; 7(1-2):27-34. http://dx.doi.org/10.1007/BF00401880.

13. Choudhury P and Agrawal DC. Sol-gel derived hydroxyapatite coatings on titanium substrates. *Surface and Coatings Technology*. 2011; 206(2-3):360-365. http://dx.doi.org/10.1016/j.surfcoat.2011.07.031.

14. Büyükşağiş A, Çiftçi N, Ergün Y and Kayali Y. The examination of corrosion behaviors of hap coated Ti implant materials and 316L SS by sol-gel method. *Protection of Metals and Physical Chemistry of Surfaces*. 2011; 47(5):670-679. http://dx.doi.org/10.1134/S2070205111050054.

15. Abdeltawab AA, Shoeib MA and Mohamed SG. Electrophoretic deposition of hydroxyapatite coatings on titanium from dimethylformamide suspensions. *Surface and Coatings Technology*. 2011; 206(1):43-50. http://dx.doi.org/10.1016/j.surfcoat.2011.06.034.

16. Wang C, Ma J, Cheng W and Zhang R. Thick hydroxyapatite coatings by electrophoretic deposition. *Materials Letters*. 2002; 57(1):99-105. http://dx.doi.org/10.1016/S0167-577X(02)00706-1.

17. Kokubo T, Hata K, Nakamura T and Yamamuro T. Apatite formation on ceramics, metals, and polymers induced by a CaO, SiO2 based glass in a simulated body fluid. In: Bonfield W, Hastings GW and Tanner KE, editors. Bioceramics: Proceedings of the 4th International Symposium on Ceramics in Medicine; 1991; Oxford, London. Oxford: Butterworth-Heinemann; 1991. p. 113-120. v. 4.

18. Paz A, Martín Y, Pazos LM, Parodi MB, Ybarra GO and González JE. Obtención de recubrimientos de hidroxiapatita sobre titanio mediante el método biomimético. *Revista de Metalurgia*. 2011; 47(2):138-145. http://dx.doi.org/10.3989/revmetalmadrid.1009.

19. Thair L, Ismaeel T, Ahmed B and Swadi AK. Development of apatite coatings on Ti–6Al–7Nb dental implants by biomimetic process and EPD: *in vivo* studies. *Surface Engineering*. 2011; 27(1):11-18. http://dx.doi.org/10.1179/174329409X439023.

20. García-Sanz FJ, Mayor MB, Arias JL, Pou J, León B and Pérez-Amor M. Hydroxyapatite coatings: a comparative study between plasma-spray and pulsed laser deposition techniques. *Journal of Materials Science. Materials in Medicine*. 1997; 8(12):861-865. http://dx.doi.org/10.1023/A:1018549720873. PMid:15348805

21. Sergo V, Sbaizero O and Clarke DR. Mechanical and chemical consequences of the residual stresses in plasma sprayed hydroxyapatite coatings. *Biomaterial*. 1997; 18(6):477-482. http://dx.doi.org/10.1016/S0142-9612(96)00147-0.

22. Nagase M, Nishiya H and Abe Y. The effect of crystallinity on hydroxyapatite-induced production of reactive oxygen metabolites by polymorphonuclear leukocytes. *FEBS Letters*. 1993; 325(3):247-250. http://dx.doi.org/10.1016/0014-5793(93)81082-B. PMid:8391480

23. Dunleavy CS, Golosnoy IO, Curran JA and Clyne TW. Characterisation of discharge events during plasma electrolytic oxidation. *Surface and Coatings Technology*. 2009; 203(22):3410-3419. http://dx.doi.org/10.1016/j.surfcoat.2009.05.004.

24. Tsui YC, Doyle C and Clyne TW. Plasma sprayed hydroxyapatite coatings on titanium substrates. Part 1: Mechanical properties and residual stress levels. *Biomaterials*. 1998; 19(22):2015-2029. http://dx.doi.org/10.1016/S0142-9612(98)00103-3. PMid:9870753

25. Tsui YC, Doyle C and Clyne TW. Plasma sprayed hydroxyapatite coatings on titanium substrates. Part 2: optimisation of coating properties. *Biomaterials*. 1998; 19(22):2031-2043. http://dx.doi.org/10.1016/S0142-9612(98)00104-5. PMid:9870754

26. Curran JA and Clyne TW. Porosity in plasma electrolytic oxide coatings. *Acta Materialia*. 2006; 54(7):1985-1993. http://dx.doi.org/10.1016/j.actamat.2005.12.029.

27. Montazeri M, Dehghanian C, Shokouhfar M and Baradaran A. Investigation of the voltage and time effects on the formation of hydroxyapatite-containing titania prepared by plasma electrolytic oxidation on Ti–6Al–4V alloy and its corrosion behavior. *Applied Surface Science*. 2011; 257(16):7268-7275. http://dx.doi.org/10.1016/j.apsusc.2011.03.103.

28. Rudnev VS, Morozova VP, Lukiyanchuk IV and Adigamova MV. Calcium-containing biocompatible oxide-phosphate coatings on titanium. *Russian Journal of Applied Chemistry*. 2010; 83(4):671-679. http://dx.doi.org/10.1134/S107042721004018X.

29. Rudnev VS, Medkov MA, Yarovaya TP and Nedozorov PM. Calcium and strontium phosphates coatings on titanium formed by the plasma electrolytic oxidation. *Russian Journal of Applied Chemistry*. 2012; 85(12):1856-1860. http://dx.doi.org/10.1134/S1070427212120117.

30. Durdu S, Deniz ÖF, Kutbay I and Usta M. Characterization and formation of hydroxyapatite on Ti6Al4V coated by plasma electrolytic oxidation. *Journal of Alloys and Compounds*. 2013; 551:422-429. http://dx.doi.org/10.1016/j.jallcom.2012.11.024.

31. Cheng T, Chen Y and Nie X. Surface morphology manipulation and wear property of bioceramic oxide coatings on titanium alloy. *Surface and Coatings Technology*. 2013; 215:253-259. http://dx.doi.org/10.1016/j.surfcoat.2012.07.093.

32. Sun J, Han Y and Huang X. Hydroxyapatite coatings prepared by micro-arc oxidation in Ca- and P-containing electrolyte. *Surface and Coatings Technology*. 2007; 201(9-11):5655-5658. http://dx.doi.org/10.1016/j.surfcoat.2006.07.052.

33. Declercq H, Van den Vreken N, De Maeyer E, Verbeeck R, Schacht E, De Ridder L, et al. Isolation, proliferation and differentiation of osteoblastic cells to study cell/biomaterial interactions: comparison of different isolation techniques and source. *Biomaterials*. 2004; 25(5):757-768. http://dx.doi.org/10.1016/S0142-9612(03)00580-5. PMid:14609664

34. Whiteside P, Matykina E, Gough JE, Skeldon P and Thompson GE. In vitro evaluation of cell proliferation and collagen synthesis on titanium following plasma electrolytic oxidation. *Journal of Biomedical Materials Research. Part A*. 2010; 94(1):38-46. http://dx.doi.org/10.1002/jbm.a.32664. PMid:20091708

35. Robinson HJ, Markaki AE, Collier CA and Clyne TW. Cell adhesion to plasma electrolytic oxidation (PEO) titania coatings, assessed using a centrifuging technique. *Journal of the Mechanical Behavior of Biomedical Materials*. 2011; 4(8):2103-2112. http://dx.doi.org/10.1016/j.jmbbm.2011.07.009. PMid:22098910

36. Yeung WK, Reilly GC, Matthews A and Yerokhin A. In vitro biological response of plasma electrolytically oxidized and plasma-sprayed hydroxyapatite coatings on Ti-6Al-4V alloy. *Journal of Biomedical Materials Research. Part B, Applied Biomaterials*. 2013; 101(6):939-949. http://dx.doi.org/10.1002/jbm.b.32899. PMid:23529912

Artigo 2

Mg-Containing Hydroxyapatite Coatings Produced by Plasma Electrolytic Oxidation of Titanium

César Augusto Antônio[a,b]*, Elidiane Cipriano Rangel[a], Steven Frederick Durrant[a], Adriana de Oliveira Delgado-Silva[c], Manfredo H. Tabacniks[d], Nilson Cristino da Cruz[a]

[a] *Laboratory of Technological Plasmas, Sorocaba Institute of Science and Technology, Paulista State University - UNESP, Sorocaba, SP, Brazil*
[b] *Sorocaba College of Technology, Sorocaba, SP, Brazil.*
[c] *Federal University of São Carlos, Sorocaba, SP, Brazil.*
[d] *Institute of Physics, University of São Paulo - USP, São Paulo, SP, Brazil.*

Plasma Electrolytic Oxidation (PEO) is promising for the processing of biomaterials because it enables the production of surfaces with adjustable composition and structure. In this work, aimed at the improvement of the bioactivity of titanium, PEO has been used to grow calcium phosphide coatings on titanium substrates. The effects of the addition of magnesium acetate to the electrolytes on the composition of the coatings produced during 120 s on Ti disks using bipolar voltage pulses and solutions of calcium and magnesium acetates and sodium glycerophosphate as electrolytes have been studied. Scanning electron microscopy, X-ray energy dispersive spectroscopy, Rutherford backscattering spectroscopy, X-ray diffractometry with Rietveld refinement and profilometry were used to characterize the modified samples. Coatings composed of nearly 50 % of Mg-doped hydroxyapatite have been produced. In certain conditions up to 4% Mg can be incorporated into the coating without any observable significant structural modifications of the hydroxyapatite.

Keywords: *Plasma Electrolytic Oxidation, Mg-doped hydroxyapatite, titanium*

1. Introduction

Owing to high biocompatibility, good corrosion and wear resistance, good mechanical properties, low density and chemical inertness, titanium and its alloys are widely used in the production of dental and orthopedic implants[1,2].

Although titanium is biocompatible[3,4], its intrinsic bioinertness does not stimulate spontaneous bone-implant integration[5]. To expand the successful applications as dental and orthopedic implants several methods are used to modify the titanium surface with the objective of improving its bioactivity. In this context, great improvement in biological properties, consequently reducing the rejection of implants[6], has been achieved with calcium phosphate coatings.

Hydroxyapatite $(Ca_{10}(PO_4)_6(OH)_2)$ (HA) is a calcium phosphate that constitutes about 70% in weight of human bones. HA is a natural mineral that has excellent biological properties. When it is synthetically produced on the surface of titanium, it can promote bioactivity and improve the connection with bone tissue[7]. Nowadays it is possible to produce synthetic HA with similar characteristics to those of human bone, including bioactivity and biocompatibility, that can be used in biomedical applications[8,9].

Over the last decade, various methods for producing HA coatings on titanium and its alloys have been developed[10-25]. These include plasma spray[10-18], sputtering[19,20], electrophoretic deposition[21,22], immersion in simulated body fluid (SBF)[23], biomimetic techniques[24], sol-gel procedures[25,26] and laser ablation[27]. There are, however, some problems related to the hydroxyapatite coatings, such as poor control of the chemical composition and structure and poor coating adhesion to the substrate[5,28-30]. Therefore, there is still a demand for methods to produce HA with greater bioactivity and similarity to human bone combined with good mechanical properties[31,32].

The absorption of nutrients and the growth of bone are improved by the presence of ions such as Zn^{+2}, Mg^{+2}, Na^+, CO_3^{-2} and F in non-stoichiometric compounds of low crystallinity[33-35]. Owing to that, improvements in the biological properties and greater similarity to human bone can be achieved by the incorporation of ionic elements into synthetic HA[36,37]. Magnesium is the fourth most abundant ion present in the human body, where it helps to inhibit crystallization, to reduce crystal size, to decrease the proliferation and activities of osteoblast-like cells[38-41]. Therefore, magnesium deficiency can affect bone metabolism and growth, reducing osteoplastic activity and resulting in fragile bones[42-46].

Plasma Electrolytic Oxidation (PEO) combines the effects of conventional electrolysis with micro-arc discharges that appear on the sample surface. When the voltage applied

between two electrodes immersed in electrolytic solutions exceeds several hundred volts, the dielectric barrier of the oxide coating produced on the metal surface at the anode is broken down mostly by impact ionizations. Consequently, many high energy micro-arcs able to melt the oxide coating arise on the surface of the sample. In this condition, chemical elements present in the electrolytic solution can be incorporated into the coating. Also, the high thermal energy from the micro-arcs can produce ceramic coatings with complex structures. This method has been successfully used to produce ceramic coatings on light weight metals such as Ti, Al, Nb, Ta and Mg[47].

Recent studies have shown that HA can be produced by PEO of titanium and its alloys. Usually, however, long process times (>20 min) or two-step procedures are required and the HA produced is of low crystallinity[48,49]. In titanium oxidation using PEO other structures such as anatase, rutile, and phosphates are also produced. Results of X-ray diffraction (XRD) studies have shown that the proportion of HA is generally low, i.e., anatase and rutile phases are predominant[50]. To our best knowledge there were no studies of the production of HA by PEO with Mg incorporation into the coating for improved bioactivity of the synthetic HA. Thus, this study aims to produce a coating on Grade 4 titanium with a high concentration of Mg-doped HA with very short treatment time.

2. Experimental description

The HA coatings were deposited on grade 4 titanium disks 8 mm in diameter and 2 mm thick. After machining and polishing, the substrates were ultrasonically cleaned and stored. Figure 1 shows schematically the treatment system. The treatments have been performed using a two liter stainless steel tank, enclosed in a cooling system that keeps the temperature of the solution constant. The substrate was connected to the positive terminal of a pulsed bipolar voltage supply and the tank itself served as the cathode. The electrolytic solution used for the treatment was prepared by diluting 0.2 M of calcium acetate and 0.02 M of sodium glycerophosphate in deionized water. The variable process parameter was the amount C_M of magnesium acetate (MgA) added in concentrations of 0.0, 0.02, 0.04, 0.06 and 0.08 M to the electrolytic solution. The samples have been biased with positive pulses of 480 V with frequency and duty cycle of 100 Hz and 60 %, respectively. The substrates were treated for 120 s in the potentiostatic mode. After PEO treatment, the samples were cleaned with distilled water and dried.

A previous study by the authors[51] concluded that a treatment time of 120 s was sufficient to produce a coating with a high HA content. Therefore, based on that study, all the other process parameters were maintained; only a different amount of MgA in the electrolytic solution was used.
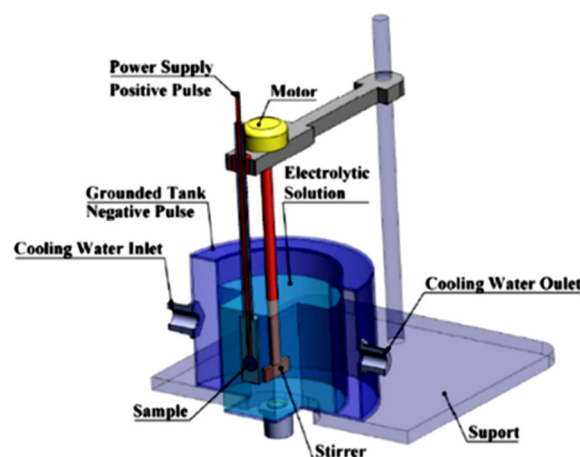

Figure 1. Schematic representation of the treatment cell.

After metallographic preparation of cross-sectioned samples, coating thickness was measured using scanning electron microscopy (SEM). Roughness was investigated using profilometry and surface morphology was examined by SEM.

The chemical composition of the samples was analyzed using Rutherford backscattering spectrometry (RBS). A He+ beam, from a Pelletron-tandem accelerator produced by National Electrostatic Corporation (NEC) model 5SDH, was directed onto the samples in a vacuum chamber at 7° incidence and 170° scattering angles. The energy of the ions was 3.29 MeV and the beam charge was 10 µC. Chemical composition and elemental depth profiles were determined by computer simulations using RUMP[52] and SIMNRA[53] softwares.

Analysis of the coating crystalline structure was based on X-ray diffraction data obtained using a Panalytical X-Pert Powder diffractometer in theta-2 theta geometry, which employed Cu-K$_a$ radiation ($\lambda = 1.54$ Å). Data acquisition was performed at diffraction angles of between 20 and 60°, using a step-size of 0.02° at 5 s per step. The Rietveld Refinement technique was employed to determinate the proportion of each phase as well as hydroxyapatite cell parameters. The refinement was performed using X'Pert HighScorePlus software with the structural model (ISCD database) listed in Table 1. The quantity of each phase was calculated, but the cell parameters were determined only for the HA phase, the main object of study in this research. The electric current through the electrolytic cell was measured with a digital amperimeter every 2 s during the treatment. Three measurements were performed for each treatment condition.

3. Results and Discussion

3.1. Current density characteristics.

Figure 2 (a) shows the current density during the treatment and the average current density after 7 s of treatment, when the voltage reached 480 V, is presented in Figure 2 (b).

Table 1. Structural model (ISCD database) of the possible phases present in the PEO coating.

| Phase	Formula	ICSD code
Anatase	TiO_2	200392
Rutile	TiO_2	36413
Titanium	Ti	43614
Calcium Phosphate	Ca_3P_8	74854
Hydroxyapatite	$Ca_5(PO_4)_3(HO)$	203027
Magnesium Phosphide	Mg_3P_2	24489
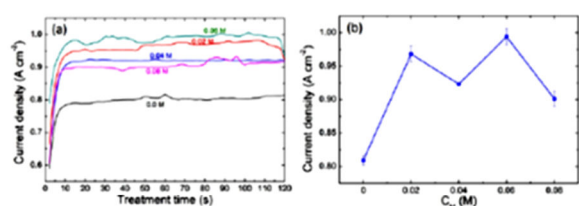
Figure 2. (a) Current density as a function of treatment time and (b) average current as a function of C_M.

In a general way, the addition of MgA to the electrolytic solutions increased the current density due to the increment of ion densities in solution. The maximum value was observed for treatments with $C_M = 0.06$ M. The current density in these treatment conditions was 0.99 (± 0.012) A cm^{-2}, which is 24% higher than the current density measured during treatments with $C_M = 0.0$ M.

Inspection of Figure 2 (b) reveals some variations in the current density, which were caused by instabilities generated by micro-arc discharges produced when the ion density was increased. The amount of MgA increased linearly but the micro-arcs occur in thermodynamic non-equilibrium and the electrolysis does not occur according to the usual electrochemical laws. Consequently, detailed explanations of the observed variations in the current densities are not available.

3.2. Thickness and roughness

The coating thicknesses were measured from MEV images of sample cross-sections prepared by metallography. Averages and standard deviations determined from measurements of the thicknesses of three samples are given. Figures 3 (left and right) show the thicknesses as a functions of C_M and typical cross-sections of samples treated by PEO. The addition of magnesium acetate to the electrolytic solutions did not change significantly the coating thickness. Samples treated in solutions with C_M up to 0.06 M had thicknesses of around 10 μm but samples treated at a C_M of 0.08 M had thicknesses of around 8.0 μm. It was also was observed that dispersion of the thickness measurements decreases when the C_M was 0.06 M. Therefore, the results show that this condition ($C_M = 0.06$ M) produced a more uniform coating because the process combined the best parameters of current density, voltage, composition of the electrolytic solution and treatment time.
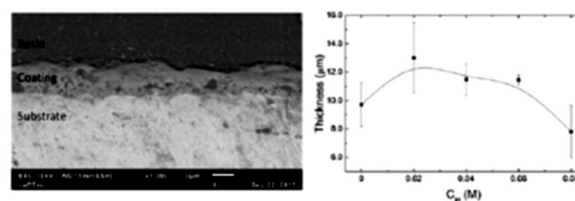

Figure 3. (left) SEM micrograph of a typical cross section of a samples treated with $C_M = 0.06$ M. (right) Thickness of the coatings as a function of C_M.

As it can be noticed in Figure 4, which shows the Ra roughness as a function of C_M, the roughness decreases with the increasing of C_M up to 0.06 M and then grows to reach 6.5 ± 1.17 μm when $C_M = 0.08$ M. This result reflects the modification of the intensities of the micro-arc as the proportion of magnesium acetate is modified.
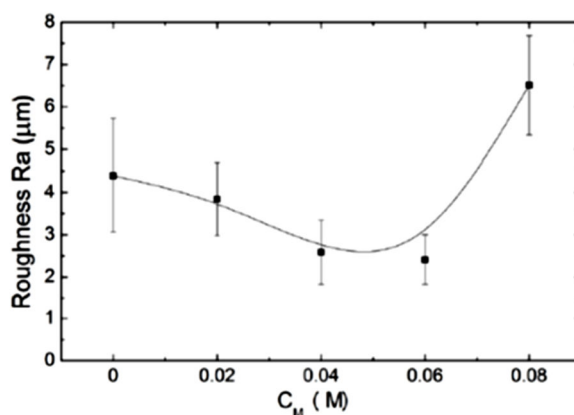
Figure 4. Roughness of titanium samples treated by PEO at different C_M.

3.3. Coating Morphology

Figure 5 presents SEM micrographs of surfaces produced in solutions with various C_M. It can be pointed out the presence of clusters of granular structures on the surface of all the samples produced with $C_M < 0.08$ M. As previously reported[53], such structures are mostly composed of hydroxyapatite. Therefore, the decrease of the density of such clusters in Figure 5 suggests that the higher C_M the lower the proportion of HA.
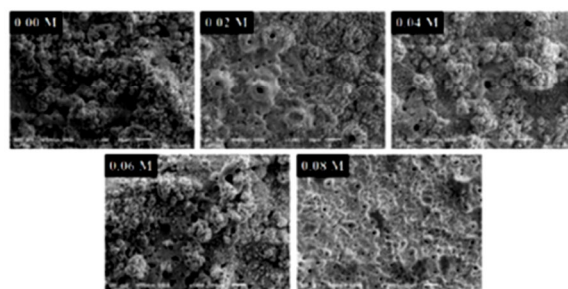
Figure 5. SEM micrographs of titanium samples treated by PEO with different C_M concentrations.

3.4. Chemical compositions

As previously noted the samples present porous irregular surfaces. As can be observed in Figure 6, which shows typical simulated and experimental RBS spectra, such rough morphology makes rather difficult the theoretical adjustment of the measured RBS spectra. Therefore, to ensure a good agreement between theoretical and experimental values, the simulations were restricted to the outermost 100 nm thick layer of all the samples. It is important to mention that the complexities of the simulations imposed by the irregular surface introduced an estimated error of about 5%.
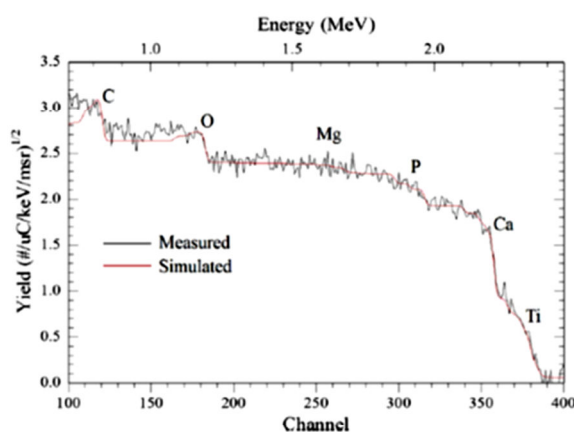

Figure 6. RBS spectrum (measured and simulated) of the sample treated by PEO with C_M = 0.06 M.

The average proportions of Ca, P, Mg, and Ti in a 100 nm thick superficial layer can be observed in Figure 7. The proportions of carbon (nearly 32%) and oxygen (approximately 47%) have been omitted since they do not provide any useful information to the discussions that follow. According to the results, the addition of MgA to the electrolytes caused the Ca concentration to decrease from 12.2 to 8.9 at%, independently of C_M. On the other hand, the concentration of phosphorous remained constant at 8.4 at% and decreased when MgA was added in proportions larger than 0.04 M reaching 1.2 at% when C_M = 0.08 M. This strong decrease can be attributed to the low boiling point of P (553.6 K), which can easily evaporate from sample surface. It has been observed the intensification of the light emitted by the micro-arcs as magnesium acetate is added to the solution. This observation associated to the higher current observed in Figure 2 indicates the enhancement of the energy transferred to the sample when MgA is added to the solution, which may cause the heating of the coating. The heating near the surface of the sample makes impedes the deposition of low melting point elements and also increases the diffusion of species to inner coating regions. Both mechanisms contribute to the observed depletion of phosphorous. In addition, the Mg concentration in the coating increased with the increasing of the proportion of magnesium acetate added to the solution,
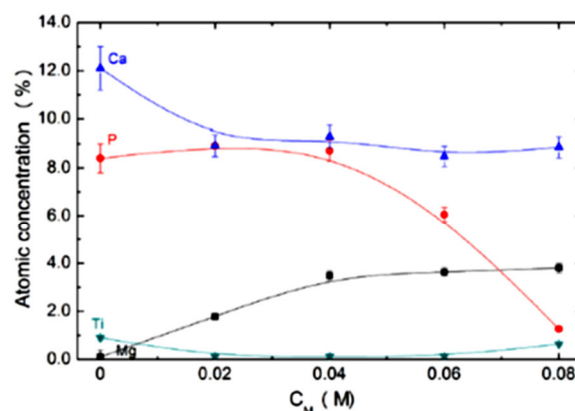

Figure 7. Average atomic proportion of elements in samples treated with different C_M determined by RBS in a 100 nm thick superficial layer.

reaching about 3.6 at% on samples treated with C_M = 0.08 M. Less than 1.0% of titanium has been detected in all the samples indicating that the electrophoretic deposition rather than the re-deposition of the quenched metal after melting by the micro-arc is the predominant mechanism of coating growth. Accordingly to the RBS analyses, the surfaces produced in this work are very promising for implants since they are mostly composed by Ca, P, and Mg.

X-ray energy dispersive spectroscopy (EDS) has been employed to evaluate the coating composition in bulk regions deeper that those probed by RBS. As can be seen in Figure 8 the concentrations are significantly different from those determine near the surface. In disagreement with what is observed near the surface, the average concentrations of Ca, P and Ti in the bulk are nearly independent of the amount of magnesium acetate added up to C_M = 0.04 M. Larger C_M caused the proportions of Ca and P to decrease. When CM = 0.08 M the proportion of Ca is 35% smaller than that measured without the addition of Mg acetate while the proportion of titanium increases fourfold with the same variation of C_M. It is interesting to mention that the proportions of calcium and phosphorous in all the conditions are roughly the same as was detected by RBS on the superficial layer of the samples produced without the addition of magnesium. This observation corroborates the supposition of the enhancement of the diffusion of species to deeper regions as a consequence of the increase of the heating caused by larger currents when the amount of MgA in the solution is increased. Moreover, larger current densities can produce micro-arcs intense enough to reach the substrate beneath the coating resulting in the ejection of molten titanium towards the liquid. The quenching of the metal by the electrolyte explains the high amount of Ti in the bulk of coatings as thick as 8 μm.

3.4. X-ray Diffraction and Rietveld Refinement.

Figure 9 shows X-ray diffraction spectra of the coatings produced with various C_M. From this figure it is possible
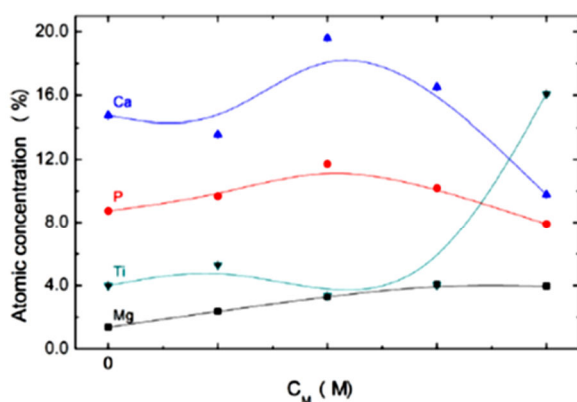
Figure 8. Atomic proportions determined by EDS in the bulk of samples treated with different C_M.

to observe that the treatments resulted in the formation of anatase, rutile, crystalline calcium phosphate, magnesium phosphides, and hydroxyapatite. The diffractograms also reveal the modification of the crystalline structure of the coatings as the proportion of magnesium acetate is increased. It is possible to conclude that the higher C_M, the smaller the peaks related to hydroxyapatite as becomes evident if one notes that diffractogram of the coating grown with $C_M = 0.08$ M contains only the peaks produced by anatase, rutile and metallic titanium.
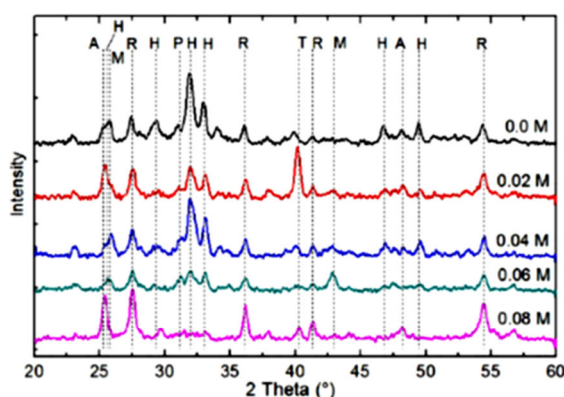

Figure 9. XRD patterns of coatings produced by PEO with different C_M, where the letters stand for: H - Hydroxyapatite; P - Calcium Phosphate, R - Rutile, M - Magnesium phosphide, A - Anatase, and T - titanium.

The phase composition of the samples can be better evaluated from the results of Rietveld refinement presented in Figure 10. The coating produced without the addition of MgA is composed by 83.5% HA, 15.9% rutile and 0.9% calcium phosphate. Samples treated with $C_M = 0.02$, 0.04, and 0.06 M are composed of around 50% hydroxyapatite. The reduction in the amount of HA can be attributed to the greater incorporation of Mg and the reduction of the proportion of phosphorous in the coatings, as shown in Figure 8. In addition, the same amount of P was bound as magnesium phosphide (Mg_3P_2).

The greatest amount of magnesium phosphide was observed in samples produced in electrolytic solutions with
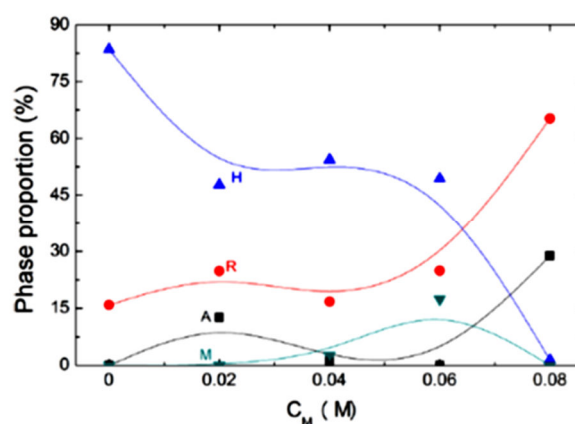

Figure 10. Phases proportion calculated by Rietveld refinement of samples treated by PEO as a function of C_M. The letters stand for: H - Hydroxyapatite, R - Rutile, M - Magnesium phosphide, and A - Anatase

$C_M = 0.06$ M. Therefore, this condition produced an ideal coating for biological applications because the composition of crystalline phases combines significant amounts of hydroxyapatite, magnesium phosphide and TiO_2 (rutile). On the other hand, the samples produced with $C_M = 0.08$ M were predominately composed by titanium (4.5%) and titanium dioxide (65.3% rutile, 28.8% anatase). No HA was formed under that condition because of the deficiency of phosphorous.

Some authors[54,55] have reported that Mg^{2+} ions can be incorporated into the crystalline structure of hydroxyapatite, replacing Ca^{2+} ions. The Mg^{2+} ions have ionic radius of 0.069 nm that is smaller than radius of Ca^{2+} ions (0.099 nm). Thus Mg^{2+} can easily replace Ca^{2+} in the crystalline structure. This effect can also reduce the lattice parameters a and c of the hexagonal crystalline structure of the HA. In the present study, it may be observed from Figure 11 that those lattice parameters did decrease when the samples were treated with $C_M = 0.02$ M and 0.04 M in comparison with samples treated without addition of MgA to the electrolyte. This effect is attributed to the replacement of Ca^{2+} by Mg^{2+} ions in the hydroxyapatite crystalline structure. The sample treated with $C_M = 0.06$ M presents the lattice parameters closer to the lattice parameters of samples treated without addition of MgA. The results of Rietveld refinement revealed that this coating contains 17.4% magnesium phosphide, the largest proportion of this phase found in this study. Therefore, most of the magnesium incorporated is present as magnesium phosphide, thus explaining why the hydroxyapatite crystalline structure is similar to the crystalline structure of the hydroxyapatite produced with $C_M = 0$.

4. Conclusion

In the present work the efficacy of PEO to produce Mg-doped HA was studied. The addition of magnesium acetate to the electrolytic solution of calcium acetate and sodium glycerophosphate allowed the production of coatings with up
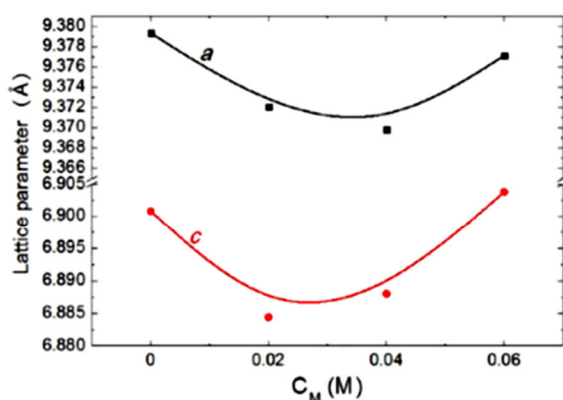
Figure 11. Hydroxyapatite lattice parameters in samples produced by PEO with various C_M.

to 50% of Mg-containing HA. Results of Rietveld refinement have shown the decrease of the lattice parameters a and c of HA crystalline structures in coatings produced in solutions with C_M = 0.02 and 0.04 M. Such characteristics suggest the replacement of Ca by Mg ions in the HA structure, confirming the production of Mg-doped HA. The treatment with the electrolyte containing 0.06 M MgA was effective in producing HA with a crystalline structure similar to that of HA produced with C_M = 0.0 M. In that case, the coating produced contained around 17% of magnesium phosphide. In conclusion, this work demonstrated the versatility of PEO since the modification of the composition of the electrolyte allowed the adjustment of the morphology, composition, and crystalline structure of the coatings. The PEO process has been demonstrated to produce a large amount of Mg-doped HA chemically bonded to the substrate in only 120 s. In addition, the coating surface is porous and rough, which are important properties for biological applications.

5. Acknowledgment

6. References

1. Albrektsson T, Brånemark PI, Hansson HA, Lindström J. Osseointegrated titanium implants. Requirements for ensuring a long-lasting, direct bone-to-implant anchorage in man. *Acta Orthopaedica Scandinavica*. 1981;52(2):155-170.

2. Long M, Rack HJ. Titanium alloys in total joint replacement-a materials science perspective. *Biomaterials*. 1998;19(18):1621-1639.

3. Sennerby L, Thomsen P, Ericson LE. Ultrastructure of the bone-titanium interface in rabbits. *Journal of Materials Science: Materials in Medicine*. 1992;3(4):262-271.

4. Steflik DE, Sisk AL, Parr GR, Gardner LK, Hanes PJ, Lake FT, et al. Osteogenesis at the dental implant interface: High-voltage electron microscopic and conventional transmission electron microscopic observations. *Journal of Biomedical Materials Research Part A*. 1993;27(6):791-800.

5. Liu F, Wang F, Shimizu T, Igarashi K, Zao L. Formation of hydroxyapatite on Ti-6Al-4V alloy by microarc oxidation and hydrothermal treatment. *Surface and Coatings Technology*. 2005;199(2-3):220-224.

6. Wong M, Eulenberger J, Schenk R, Hunziker E. Effect of surface topology on the osseointegration of implant materials in trabecular bone. *Journal of Biomedical Materials Research*. 1995;29(12):1567-1575.

7. Fatehi K, Moztarzadeh F, Solati-Hashjin M, Tahriri M, Rezvannia M, Ravarian R. *In vitro* biomimetic deposition of apatite on alkaline and heat treated Ti6Al4V alloy surface. *Bulletin of Materials Science*. 2008;31:101-108.

8. Halouani R, Bernache-Assolant D, Champion E, Ababou A. Microstructure and related mechanical properties of hot pressed hydroxyapatite ceramics. *Journal of Materials Science: Materials in Medicine*. 1994;5(8):563-568.

9. Thomas MB, Doremus RH. Fracture strength of dense hydroxylapatite. *American Ceramic Society Bulletin*. 1981;60(2):258-259.

10. Vijayaraghavan TV, Bensalem A. Electrodeposition of apatite coating on pure titanium and titanium alloys. *Journal of Materials Science Letters*. 1994;13(24):1782-1785.

11. Weng W, Baptista JL. Preparation and Characterization of Hydroxyapatite Coatings on Ti6Al4V Alloy by a Sol-Gel Method. *Journal of the American Ceramic Society*. 1999;82(1):27-32.

12. Nishio K, Neo M, Akiyama H, Nishiguchi S, Kim HM, Kokubo T, et al. The effect of alkali- and heat-treated titanium and apatite-formed titanium on osteoblastic differentiation of bone marrow cells. *Journal of Biomedical Materials Research*. 2000;52(4):652-661.

13. Wang CK, Lin JH, Ju CP, Ong HC, Chang RP. Structural characterization of pulsed laser-deposited hydroxyapatite film on titanium substrate. *Biomaterials*. 1997;18(20):1331-1338.

14. Yang B, Uchida M, Kim HM, Zhang X, Kokubo T. Preparation of bioactive titanium metal via anodic oxidation treatment. *Biomaterials*. 2004;25(6):1003-1010.

15. Lim YM, Park YJ, Yun YH, Hwang KS. Functionally graded Ti/HAP coatings on Ti-6Al-4V obtained by chemical solution deposition. *Ceramics International*. 2002;28(1):37-41.

16. Yang S, Man HC, Xing W, Zheng X. Adhesion strength of plasma-sprayed hydroxyapatite coatings on laser gas-nitrided pure titanium. *Surface and Coatings Technology*. 2009;203(20-21):3116-3122.

17. Kozerski S, Pawlowski L, Jaworski R, Roudet F, Petit F. Two zones microstructure of suspension plasma sprayed hydroxyapatite coatings. *Surface and Coatings Technology*. 2010;204(9-10):1380-1387.

18. d'Haese R, Pawlowski L, Bigan M, Jaworski R, Martel M. Phase evolution of hydroxapatite coatings suspension plasma sprayed using variable parameters in simulated body fluid. *Surface and Coatings Technology*. 2010;204(8):1236-1246.

19. Chen S, Liu W, Huang Z, Liu X, Zhang Q, Lu X. The simulation of the electrochemical cathodic Ca-P deposition process. *Materials Science and Engineering: C*. 2009;29(1):108-114.

20. Blackwood DJ, Seah KHW. Electrochemical cathodic deposition of hydroxyapatite: improvements in adhesion and crystallinity. *Materials Science and Engineering: C.* 2009;29(4):1233-1238.

21. Wang J, Huang C, Wan Q, Chen Y, Chao Y. Characterization of fluoridated hydroxyapatite/zirconia nano-composite coating deposited by a modified electrocodeposition technique. *Surface and Coatings Technology.* 2010;204(16-17):2576-2582.

22. Yang X, Zhang B, Lu J, Chen J, Zhang X, Gu Z. Biomimetic Ca-P coating on pre-calcified Ti plates by electrodeposition method. *Applied Surface Science.* 2010;256(9):2700-2704.

23. Long LH, Chen LD, Bai SQ, Chang J, Lin KL. Preparation of dense β-CaSiO$_3$ ceramic with high mechanical strength and HAp formation ability in simulated body fluid. *Journal of the European Ceramic Society.* 2006;26(9):1701-1706.

24. Zhang E, Zou C, Zeng S. Preparation and characterization of silicon-substituted hydroxyapatite coating by a biomimetic process on titanium substrate. *Surface and Coatings Technology.* 2009;203(8):1075-1080.

25. Cheng K, Zhang S, Weng W, Zeng X. The interfacial study of sol-gel-derived fluoridated hydroxyapatite coatings. *Surface and Coatings Technology.* 2005;198(1-3):242-246.

26. Zhang S, Zeng X, Wang Y, Cheng K, Weng W. Adhesion strength of sol-gel derived fluoridated hydroxyapatite coatings. *Surface and Coatings Technology.* 2006;200(22-23):6350-6354.

27. Hu J, Wang Z, Guan T, Gao Y, Lv X, Lin X, et al. In situ synthesis and fabrication of tricalcium phosphate bioceramic coating on commercially pure titanium by laser rapid forming. *Surface and Coatings Technology.* 2010;204(23):3833-3837.

28. Wang BC, Chang E, Lee TM, Yang CY. Changes in phases and crystallinity of plasma-sprayed hydroxyapatite coatings under heat treatment: A quantitative study. *Journal of Biomedical Materials Research.* 1995;29(12):1483-1492.

29. Kangasniemi IM, Verheyen CC, van der Velde EA, de Groot K. In vivo tensile testing of fluorapatite and hydroxylapatite plasma-sprayed coatings. *Journal of Biomedical Materials Research.* 1994;28(5):563-572.

30. Liu F, Wang F, Shimizu T, Igarashi K, Zhao L. Hydroxyapatite formation on oxide films containing Ca and P by hydrothermal treatment. *Ceramics International.* 2006;32(5):527-531.

31. Jahangir AA, Nunley RM, Mehta S, Sharan A; the Washington Health Policy Fellows. *Bone graft substitutes in orthopaedic surgery.* AAOS Now; 2008. Available from: <http://www.aaos.org/news/aaosnow/jan08/reimbursement2.asp>. Access in: 06/03/2027.

32. Bose S, Tarafder S. Calcium phosphate ceramic systems in growth factor and drug delivery for bone tissue engineering: a review. *Acta Biomaterialia.* 2012;8(4):1401-1421.

33. Elliott JC. Structure and Chemistry of the Apatite and Other Calcium Orthophosphates. In: Elliot JC, ed. *Studies in Inorganic Chemistry.* Amsterdam: Elsevier; 1994. p. 111-189.

34. Mayer I, Featherstone JDB. Dissolution studies of Zn-containing carbonated hydroxyapatites. *Journal of Crystal Growth.* 2000;219(1-2):98-101.

35. Abdelkader SB, Khatetech I, Rey C, Jemal M. Synthese, caractérisation et thermochimie d'apatites calco-magnésiennes hydroxylées et fluorées. *Thermochimica Acta.* 2001;376(1):25-36.

36. Narasaraju TSB, Phebe DE. Some physico-chemical aspects of hydroxyapatite. *Journal of Materials Science.* 1996;31(1):1-21.

37. Gaines RV, Skinner HCV, Foord EF, Mason B, Rosenzweig A. *Dana's New Mineralogy.* Hoboken: Wiley; 1997.

38. Sun ZP, Ercan B, Evis Z, Webster TJ. Microstructural, mechanical, and osteocompatibility properties of Mg2+/F- doped nanophase hydroxyapatite. *Journal of Biomedical Materials Research. Part A.* 2010;94(3):806-815.

39. Bigi A, Falini G, Foresti E, Ripamonti A, Gazzano M, Roveri N. Magnesium influence on hydroxyapatite crystallization. *Journal of Inorganic Biochemistry.* 1993;49(1):69-78.

40. TenHuisen KS, Brown PW. Effects of magnesium on the formation of calcium deficient hydroxyapatite from CaHPO$_4$.2H$_2$O and Ca$_4$(PO$_4$)$_2$O. *Journal of Biomedical Materials Research.* 1997;36(3):306-314.

41. Le Geros RZ. Calcium phosphates in oral biology and medicine. *Monographs in Oral Science.* 1991;15:1-201.

42. Percival M. Bone health & osteoporosis. *Applied Nutritional Science Reports.* 1999;5(4):1-6.

43. Yasukawa A, Ouchi S, Kandori K, Ishikawa T. Preparation and characterization of magnesium-calcium hydroxyapatites. *Journal of Materials Chemistry.* 1996;6(8):1401-1405.

44. Okazaki M. Crystallographic behavior of fluoridate hydroxyapatites containing Mg^{2+} and CO$^{2-}_3$ Ions. *Biomaterials.* 1991;12(9):831-835.

45. Kim SR, Lee JH, Kim YT, Riu DH, Jung SJ, Lee YJ, et al. Synthesis of Si, Mg, substituted hydroxyapatites and their sintering behaviors. *Biomaterials.* 2003;24(8):1389-1398.

46. Rude RK, Gruber HE. Magnesium deficiency and osteoporosis: animal and human observations. *The Journal of Nutritional Biochemistry.* 2004;15(12):710-716.

47. Yerokhin AL, Nie X, Leyland A, Matthews A. Characterisation of oxide films produced by plasma electrolytic oxidation of a Ti-6Al-4V alloy. *Surface and Coatings Technology.* 2000;130(2-3):195-206.

48. Durdu S, Deniz ÖF, Kutbay I, Usta M. Characterization and formation of hydroxyapatite on Ti6Al4V coated by plasma electrolytic oxidation. *Journal of Alloys and Compounds.* 2013;551:422-429.

49. Ziani S, Meski S, Khireddine H. Characterization of Magnesium-Doped Hydroxyapatite Prepared by Sol-Gel Process. *International Journal of Applied Ceramic Technology.* 2014;11(1):83-91.

50. Durdu S, Usta M. The tribological properties of bioceramic coatings produced on Ti6Al4V alloy by plasma electrolytic oxidation. *Ceramics International.* 2014;40(2):3627-3635.

51. Antônio CA, Cruz NC, Rangel EC, Rangel RCC, Araujo TES, Durrant SF, et al. Hydroxyapatite coating deposited on grade 4 Titanium by Plasma Electrolytic Oxidation. *Materials Research.* 2014;17(6):1427-1433.

52. Doolittle LR. Algorithms for the rapid simulation of Rutherford backscattering spectra. *Nuclear Instruments and Methods in*

Physics Research Section B: Beam Interactions with Materials and Atoms. 1985;9(3):344-351.

53. Markina E, Mayer M, Lee HT. Measurement of He and H depth profiles in tungsten using ERDA with medium heavy ion beams. *Nuclear Instruments and Methods in Physics Research Section B: Beam Interactions with Materials and Atoms.* 2001;269(24):3094-3097.

54. Okazaki M, LeGeros RZ. Crystallographic and chemical properties of Mg-containing apatites before and after suspension in solutions. *Magnesium Research.* 1992;5(2):103-108.

55. Landi E, Tampieri A, Mattioli-Belmonte M, Celotti C, Sandri M, Gigante A, et al. Biomimetic Mg-and Mg,CO$_3$-substituted hydroxyapatites: synthesis characterization and in vitro behavior. *Journal of the European Ceramic Society.* 2006;26(13):2593-2601.

DISCUSSÃO DOS ARTIGOS

O estudo descrito no primeiro artigo comprovou que a técnica PEO foi eficaz na produção de revestimentos com elevados teores de HA sobre o titânio. Resultados de DRX mostraram que 120 s de tratamento foram suficientes para produzir um revestimento contendo 83,5% de HA, sendo este o maior valor obtido nessa pesquisa. Os testes de viabilidade celular mostraram que as amostras tratadas por 120 s apresentaram maior capacidade de adesão e proliferação celulares, confirmando a biocompatibilidade da camada produzida. Por outro lado, observou-se a redução da quantidade de células aderidas sobre a amostra tratada por 600 s. Após 5 dias, no poço de cultivo dessas amostras, foram observadas partículas que se desprenderam do revestimento e que provavelmente contribuíram para a diminuição do crescimento celular nesta situação. Desta forma, os resultados sugerem que a amostra tratada por 120s possui características interessantes no ponto vista da produção de revestimento bioativo em comparação com o titânio não tratado.

Conforme descrito no artigo 2, mantendo-se os parâmetros de tratamento do artigo 1 e adicionando acetato de magnésio como uma fonte de íons de Mg à solução eletrolítica foi possível produzir HA dopada com Mg. Embora a adição de acetato de magnésio à solução promoveu aumento na densidade de corrente, o aumento da proporção deste elemento no eletrólito resultou na redução da espessura do revestimento. Os resultados do refinamento Rietveld dos difratogramas das amostras produzidas com a dopagem de Mg, mostraram que os revestimentos continham até 73,5% de HA dopada. A quantidade de HA no revestimento diminuiu com a adição de Mg, pois isto resultou na diminuição do teor de fósforo nos revestimentos.

CONCLUSÕES GERAIS

O presente estudo mostrou que a técnica PEO foi eficiente no processo de deposição de revestimentos contendo alto teor de hidroxiapatita sobre amostras de titânio, com tempos de tratamento curtos e sem a necessidade de pré- ou pós-tratamentos. Foram produzidos revestimentos contendo até 83,5% de hidroxiapatita com superfícies porosas e rugosas. Quantificações de fosfatase alcalina mostraram que os revestimentos de HA aumentaram em até 43% (Apêndice A Fig. 2) a diferenciação celular em comparação com o titânio não tratado.

Quando acetato de magnésio foi adicionado ao eletrólito foram obtidos revestimentos com até 73,5% de HA dopada com Mg em uma única etapa de tratamento.

REFERÊNCIAS

ADAMOPOULOS, Othon; PAPADOPOULOS, Triantafillos. Nanostructured bioceramics for maxillofacial applications. **Journal of Materials Science: Materials in Medicine**, v. 18, n. 8, p. 1587-1597, 2007.

CHEN, Yanming; MIAO, Xigeng. Thermal and chemical stability of fluorohydroxyapatite ceramics with different fluorine contents. **Biomaterials**, v. 26, n. 11, p. 1205-1210, 2005.

DOMÍNGUEZ-TRUJILLO, Cristina. et al. Sol-gel deposition of hydroxyapatite coatings on porous titanium for biomedical applications. **Surface and Coatings Technology**, v. 333, p. 158-162, 2018.

ELLIOTT, James Cornelis. Structure and chemistry of the apatites and other calcium orthophosphates. **Elsevier**, 2013.

HALOUANI, R. et al. Microstructure and related mechanical properties of hot pressed hydroxyapatite ceramics. **Journal of Materials Science: Materials in Medicine**, v. 5, n. 8, p. 563-568, 1994.

HEANEY, Robert P. Role of dietary sodium in osteoporosis. **Journal of the American College of Nutrition**, v. 25, n. sup3, p. 271S-276S, 2006.

FATEHI, K. et al. In vitro biomimetic deposition of apatite on alkaline and heat treated Ti6A14V alloy surface. **Bulletin of Materials Science**, v. 31, n. 2, p. 101, 2008.

FINI, M. et al. Biomechanical and histomorphometric investigations on two morphologically differing titanium surfaces with and without fluorohydroxyapatite coating: an experimental study in sheep tibiae. **Biomaterials**, v. 24, n. 19, p. 3183-3192, 2003.

LEWIS, Gladius. Nanostructured Hydroxyapatite Coating on Bioalloy Substrates: Current Status and Future Directions. **Journal of Advances in Nanomaterials**, v. 2, n. 1, 2017.

MARCHI, Juliana et al. Influence of synthesis conditions on the characteristics of biphasic calcium phosphate powders. **International Journal of Applied Ceramic Technology**, v. 6, n. 1, p. 60-71, 2009.

MAYER, I.; FEATHERSTONE, J. D. B. Dissolution studies of Zn-containing carbonated hydroxyapatites. **Journal of Crystal Growth**, v. 219, n. 1-2, p. 98-101, 2000.

MRÓZ, Waldemar., et al. Characterization of calcium phosphate coatings doped with Mg, deposited by pulsed laser deposition technique using ArF excimer laser. **Micron**, v. 40, n. 1, p. 140-142, 2009.

MRÓZ, Waldemar., et al. Structural studies of magnesium doped hydroxyapatite coatings after osteoblast culture. **Journal of Molecular Structure,** v. 977, n. 1-3, p. 145-152, 2010.

NARASARAJU, T. S. B.; PHEBE, D. E. Some physico-chemical aspects of hydroxylapatite. **Journal of Materials Science**, v. 31, n. 1, p. 1-21, 1996.

SHARIFNABI, Ali et al. Synthesis and characterization of nanosized magnesium-doped fluorapatite powder and coating for biomedical application. **Journal of Sol-Gel Science and Technology**, v. 74, n. 1, p. 66-77, 2015.

STIPNIECE, Liga et al. Characterization of Mg-substituted hydroxyapatite synthesized by wet chemical method. **Ceramics International**, v. 40, n. 2, p. 3261-3267, 2014.

THOMAS, M. B.; DOREMUS, R. H. Fracture strength of dense hydroxylapatite. **AM. Ceram. Soc. Bull. Am. Ceram. Soc. Bull.**, v. 60, n. 2, p. 258, 1981.

YEROKHIN, A. L. et al. Characterisation of oxide films produced by plasma electrolytic oxidation of a Ti–6Al–4V alloy. **Surface and Coatings Technology**, v. 130, n. 2-3, p. 195-206, 2000.

APÊNDICE

ANÁLISES DE BIOATIVIDADES
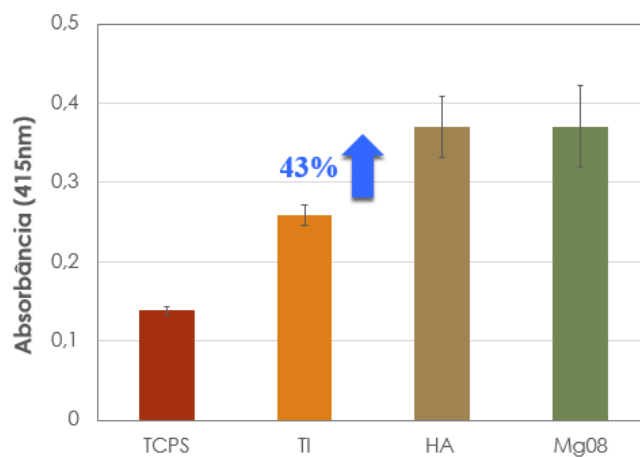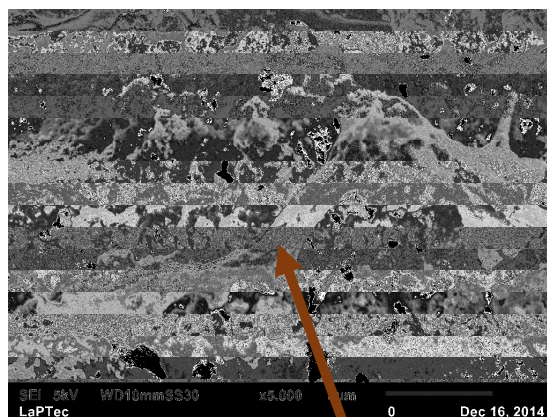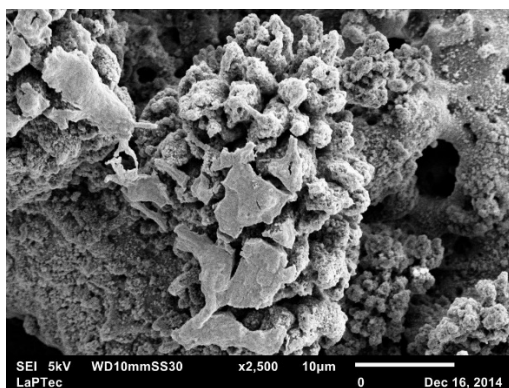
Figura 2: Resultados do ensaio de Fosfatase Alcalina

Figura 3: Imagens de células que cresceram sobre a superfície da amostra tratada com 0.6 mol de Mg, após 7 dias de cultivo. As imagens representam diferente regiões da mesma amostra.

Célula espraiada